BERICHTE
aus dem MARUM und dem Fachbereich Geowissenschaften der Universität Bremen

No. 312

Kopf, A., Fleischmann, T.,

Gauchery, T., Meinecke, G., Renken, J., Spiesecke, U., Stange, N., Völker, D., von Wahl, T., Wenau, S., Wittauer, C., Wu, T.-W.

Report and preliminary results of R/V POSEIDON cruise POS500

LISA

Ligurian Slope AUV mapping, gravity coring and seismic reflection

Catania (Italy) – Malaga (Spain)
25.05.2016 – 09.06.2016

Berichte, MARUM – Zentrum für Marine Umweltwissenschaften, Fachbereich Geowissenschaften, Universität Bremen, No. 312, 58 pages, Bremen 2016

ISSN 2195-9633

Berichte aus dem MARUM und dem Fachbereich Geowissenschaften der Universität Bremen

published by

MARUM – Center for Marine Environmental Sciences
Leobener Strasse, 28359 Bremen, Germany
www.marum.de

and

Fachbereich Geowissenschaften der Universität Bremen
Klagenfurter Strasse, 28359 Bremen, Germany
www.geo.uni-bremen.de

The "Berichte aus dem MARUM und dem Fachbereich Geowissenschaften der Universität Bremen" appear at irregular intervals and serve for the publication of cruise, project and technical reports arising from the scientific work by members of the publishing institutions.

Citation:

Kopf, A., Fleischmann, T., Gauchery, T., Meinecke, G., Renken, J., Spiesecke, U., Stange, N., Völker, D., von Wahl, T., Wenau, S., Wittauer, C., Wu, T.-W.: Report and preliminary results of R/V POSEIDON cruise POS500, LISA, Ligurian Slope AUV mapping, gravity coring and seismic reflection, Catania (Italy) – Malaga (Spain), 25.05.2016 – 09.06.2016. Berichte, MARUM – Zentrum für Marine Umweltwissenschaften, Fachbereich Geowissenschaften, Universität Bremen, No. 312, 58 pages. Bremen, 2016. ISSN 2195-9633.

An electronic version of this report can be downloaded from:
http://nbn-resolving.de/urn:nbn:de:gbv:46-MARUM9

Please place requests for printed copies as well as editorial concerns with reports@marum.de

BERICHTE AUS DEM MARUM UND DEM FACHBEREICH GEOWISSENSCHAFTEN
DER UNIVERSITÄT BREMEN

Report and preliminary results of R/V POSEIDON cruise POS500

LISA

Ligurian Slope AUV mapping, gravity coring and seismic reflection

Catania (Italy) – Malaga (Spain)
25.05.2016 – 09.06.2016

Kopf, A., Fleischmann, T.

Gauchery, T., Meinecke, G., Renken, J., Spiesecke, U., Stange, N., Völker, D.,
von Wahl, T., Wenau, S., Wittauer, C., Wu, T.-W.

2016

Table of Contents

Preface

Expedition Pos500 *LISA* (Ligurian Slope AUV mapping, gravity coring and seismic reflection) aims to shed light on the controls of slope failure and submarine landslide processes at the Ligurian Margin in the proximity of the Nice international airport, southern France. The cruise was a follow-up project of several earlier expeditions in the same area (Kopf et al., 2008, 2009; Sultan et al., 2008) and put special focus on the acquisition of high-resolution geophysical data as well as additional coring to deepen the knowledge regarding the causes of the 1979 Nice airport landslide and tsunami. The proposal is further dedicated to support a recently submitted IODP (International Ocean Discovery Program) and ICDP (International Continental Drilling Project) amphibious drilling proposal (#796-ADP by Kopf et al., 2015) and test state-of-the-art technology for long-term monitoring.

The Nice area represents an ideal natural laboratory, because a major landslide occurred in October 1979, which was well documented at the time and intensely studied thereafter. A combination of triggers was identified to have been responsible for catastrophic failure, and those triggers are currently monitored with shallow probes (<10 m below seafloor). Repeated research cruises led by MARUM Bremen or one of our French partners (IFREMER, Cerege) unraveled parts of the regional geology, in particular through Chirp surveys (Cerege) and MCS profiling (Bremen). To date, however, no high-resolution bathymetry is available for the neighbourhood of the proposed drill sites and the seafloor cable and node(s), so that we propose in the LISA cruise to carry out the following tasks: (i) detailed AUV bathymetric survey including subbottom profiling in the study area, (ii) additional high resolution MCS survey to image the delta sequences around the 1979 failure scar better, and (iii) additional gravity coring and bottom water sampling in strategic locations to acquire additional data and identify the effect of the Var aquifer in landslide triggering. Such data will be of utmost relevance to reiterate where (and when) submarine groundwater seepage is found and if/where active sediment deformation is currently taking place.

Personnel aboard R/V *Poseidon*

POS500 science party (L-R): Nikolas Stange, Tugdual Gauchery, Stefan Wenau, David Völker, Ting-Wei Wu, Christian Wittauer, Timo Fleischmann.
Not shown are Gerrit Meinecke, Achim Kopf, Jens Renken, Ulli Spiesecke, Till von Wahl.

Participating institutions

DFG-Research Centre & Cluster of Excellence MARUM
University Bremen
Leobener Strasse 2
28359 Bremen --- GERMANY

University of Bremen
Klagenfurter Strasse
28359 Bremen --- GERMANY

IFREMER
B.P. 70
29280 Plouzané --- FRANCE

1. Abstract

Cruise POS500 "LISA" with R/V *Poseidon* studied the western Ligurian Margin off Southern France, an area in the northeastern part of the western Mediterranean Sea characterized by its active tectonism and frequent mass wasting. The region near the Var estuary close to the city of Nice is particularly suited for landslide research because it represents a natural laboratority where it is possible to study a series of trigger processes of geological and anthropogenic origin. The aim of this MARUM expedition was to:

i. Study fresh water seepage in the marine Nice airport landslide and adjacent stable plateau in 15-50 m water depth using water sampling, CTD and geochemistry;
ii. Recover and deploy a number of observatories that monitor, pressure, temperature, tilt and seismicity;
iii. Run an AUV micro-bathymetric survey with MARUM AUV SEAL5000 to complement existing multibeam maps; and
iv. Acquire additional high-resolution seismic reflection profiles to unravel the complex architecture of the Nice slope and Var delta.

In a period of approximately two weeks, we acquired valuable geophysical information that helps to understand the evolution of this portion of the Ligurian Margin and further to support an active Amphibious Drilling proposal submitted to ICDP and IODP. We could also show that heavy spring rainfall plus melt water from the French Maritime Alps supplied sufficient hydraulic forcing to push Var aquifer groundwaters to seep into the marine deposits and water column. Freshening was strongest in the 1979 Nice landslide scar, but was also found at the outer edge of the shelf. Recovery and redeployment of various observatory prototypes worked well, both for the MARUM MeBo seafloor drillstring tolos and independent piezometers.

Observatory data have yet to be evaluated. In addition, geochemical analyses of bottom waters and pore waters was deferred to shore-based laboratorios except for salinity estimates using a refractometer. Seismic processing was started onboard, but is largely taking place post-cruise at University Bremen.

2. Introduction

There is a number of geological processes that pose a considerable hazard on the environment, and landslides and other mass wasting events are arguably among the most devastating ones. In fact, many of the major hazards such as volcanic eruptions or large earthquakes are often associated with flank collapses, rock falls or landslides, as well as minor mass wasting events. Onshore as well as offshore infrastructure is extremely vulnerable to these mass wastings, so that recent attention to such societal threats has increased. The stability of sediment at continental margins is a function of the intrinsic strength of the material and forces counteracting this strength (e.g. Hampton & Lee 1996). When broken down to the particle scale, the strength is controlled by the friction coefficient for the individual mineral particles at a given confining stress, minus the pore pressure that is compensating for some of the external stress. This relationship, known as the effective stress (Terzaghi 1925), is a crucial aspect in slope stability since pore pressures may equal the overburden stress, exceed lithostatic values, and hence cause liquefaction (in coarse-grained sediment) or softening (in fine-grained material) by destroying the particle network (e.g. Maltman 1994; Moore et al. 1995). Both progressive soft sediment deformation (creeping, slumping, liquefaction) as well as brittle failure (faulting, hydrofracture) are important processes in mass wasting. Slope failure is generally controlled by long-term governing factors and short-term triggers (Bjerrum 1967; Leroueil 2001; Petley et al. 2005). The first include topographic effects such as slope gradient, the geodynamic evolution of the margin (sedimentary or tectonic loading, unroofing, erosion, etc.) or other effects (glacial loading/unloading, marine transgression/regression, etc.; Lee 2009). The second group of trigger mechanisms act at a much shorter time-scale and usually cause a significant change in stress state. Among the processes most crucial to slope stability are (i) seismic loading (i.e. earthquakes), (ii) storm wave loading, (iii) rapid sedimentation (in deltas, through mass wasting, etc.), (iv) gas hydrate dissociation, (v) deep-seated fluid generation, upward migration and seepage, (vi) oversteepening, (vii) cyclic loading by tides, (viii) gas charging, and (ix) groundwater charging (see Locat & Lee 2002 for details on many of those points).

In the area of proposed research, the Ligurian coast near Nice, France, five of the above trigger mechanisms prevail and may be distinguished with an array of onshore and offshore instruments (Stegmann et al. 2011). Given that this area is highly vulnerable because of its high population density, wealth of insured capital, and the recent 1979 catastrophic event, it seems timely to equip this dynamic, groundwater-charged, metastable margin with

monitoring devices. Such monitoring in boreholes is usually expensive, but becomes affordable in the Var valley setting with access to the necessary infrastructure and very shallow coastal/marine targets. We will outline the overall scientific goals as well as the specific strategy to realise scientific drilling and long-term monitoring

At their recent meeting in Potsdam (fall 2013), representatives of ICDP recognised that none of the previous, ongoing or anticipated drilling campaigns addresses landslides or similar processes. In fact, the majority of the geohazard campaigns in ICDP are addressing seismogenic faults (SAFOD, Chelungpu, Corinth Rift, Alpine Fault, to name just a few) while a landslide has never been targeted. Similarly, IODP has very rarely targeted sites where slope stability was a main goal (except for Gulf of Mexico and Antilles drilling), so that an transect to study the hydrology and slope stability in the Var valley near Nice, France at the Ligurian coast was the natural thing to submit to foster ICD-IODP collaboration. There has been a proposal submitted to IODP that was positively evaluated IODP, which was followed by an ICDP sketch that was received favourably by the Executive Committee and will turned into a full proposal in January 2015. Also, collaborative work with the local authorities in France (departement Alpes Maritimes) onshore and EMSO (European Multi-disciplinary Seafloor Observatory) offshore sets the stage for a successful collaborative project with international visibility. Such an approach across disciplines as well as the boundary between land and sea could be beneficial for all communities involved and will help to address a number of interesting hydrogeological questions applicable to both wider parts of Liguria, but also other margins in the North Atlantic region.

2.1 Significance of Mass wasting processes

There are regions on Earth where wide stretches of ocean margins provide evidence for mass flows at many scales and over a wide range of water depths (e.g. Maslin et al. 2004; Lee 2009). Spatially, slides are a global phenomenon occurring in fjords, river deltas and fan-canyon systems, open continental slopes and volcanic flanks (e.g. Huehnerbach & Masson 2004). Submarine landslides range greatly in their size, from small, frequently occurring failures in active environments such as coastal zones and canyons, to failures that involve hundreds of km^3 of sediment but occur much more infrequently. Those megaslides (involving >1000 km^2 in area and several 100 km^3 of sediment) are commonly related to gas hydrate dissociation (e.g. the Storegga slide off Norway [Solheim et al. 2005, and refs. therein], or examples along the North Atlantic margin [Maslin et al. 2004; Lee 2009]), and

to volcanic flank collapses (Nuuanu slide off Hawaii, Canary islands). In places, landslides represent a major geohazard for offshore infrastructure (platforms, pipelines, cables and submarine installations; e.g. Sultan et al., 2004) and, if tsunamigenic, to coastal structures and populations, both locally and in the far-field (Tappin et al. 2001).

Many of the known slide events occurred a long time ago, are poorly documented, and located in remote places. Within and around Europe (Mediterranean Sea and North Atlantic/Arctic Ocean), the situation is somewhat different. The Mediterranean Sea represents a region of geodynamic diversity where mass wasting processes of various kinds are well documented from historical tradition and modern research, and are readily accessible for scientific investigation. With 46000 km of coastline, 160 Mill people along it (plus an additional 135 Mill tourists each year, i.e. 30% of the global tourism), landslides pose a considerable risk for the Mediterranean coast. Mass wasting has been reported from many of the large estuaries and delta systems in both the Eastern and Western Mediterranean (e.g. Ebro, Rhone, Var, and the Nile deep sea fan), the seismogenic Algerian or Ligurian margins, and the Mediterranean Ridge and Cretan margin further east.

In the North Atlantic sector (incl. the Nordic Seas and Mediterranean Sea), numerous large landslides have been reported for the past 45 ka, most likely associated with their proximity to massive Quarternary ice sheets (Maslin et al., 2004). The collation reveals that many events relate to periods of enhanced methane release (Preboreal and Bølling-Ållerod periods) or to sealevel lowstand (i.e. correlation of slides with Heinrich events). Although Maslin et al. (2004) argue that the latter failures were driven by lowered hydrostatic pressure as a consequence of isostatic rebound and associated seismicity after the onset of deglaciation, an equally valid explanation could be that aquifer systems utilizing porous, horizontal to gently seaward-dipping delta/prodelta deposits from glacial time may have been maintained during deglaciation and associated increase in continental wetness, or alternatively may have stepped upward in the coastal sedimentary successions. This phenomenon is not restricted to the Atlantic, but globally relevant, and may explain that many headwalls of known landslides occur in such sediments not far seaward from modern shorelines. Owing to such proximity to shore, the potential slope failures pose considerable threat to human settlements and other infrastructure along the coast.

3. Geological background

3.1 Geological setting and Regional geology

3.1.1 General setting and tectonic evolution

The Ligurian Sea is a 160-250 km wide basin in the western part of the Mediterranean Sea, which is characterized tectonically by the collision of the African and the Eurasian plates and the affects of the closure of the Tethyan Ocean and Alpine orogeny (Fig. 1). The basin formed by marginal backarc extension during the Upper Oligocene-Miocene by a drifting-rifting episode related to the Alpine-Apennine orogeny behind the Apulian subduction zone (Rehault et al. 1984). Drift of the Corsica-Sardinian block and formation of the Appennines, the latter ranging until the early Miocene, are major consequences.

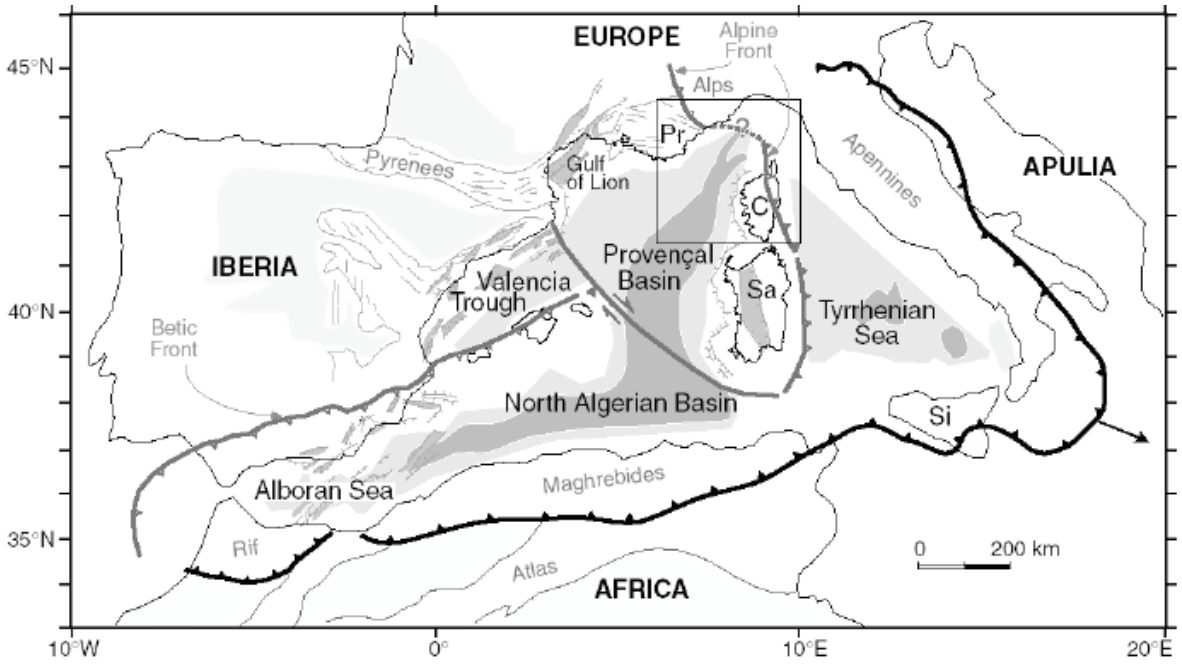

Fig. 1: Top map shows a tectonic scheme of the western Mediterranean: Active extension has shifted eastward through time, following the rollback of the Ionian-Apulian subduction zone (thick solid line). The eastward migration of the Apennines trench and the back-arc extension is symbolised by the arrow (from Rollet et al. 2002). The lower map (next page) shows the Nice Slope study area with the path of the well-documented 1979 Nice avalanche (from Mulder et al. 1997). Dashed lines show torn telecommunication cables. The location of the Marcel fault, the only prominent feature capable of producing EQs of significant magnitude, runs coast-parallel north of the Middle fan valley.

The western margin, which is the focus of the proposed drilling, is underlain by continental crust that is cross-cut by pervasive faults of reverse or transgressive type. A number of offshore lineaments are actively deforming at small deformation rates of around 1.1 m/kyr (Bethoux et al. 1998), with earthquake magnitudes commonly < M2.2-4.5 (Rehault et al. 1984) (see Fig. 2). Located within the southern subalpine fold and thrust belts (Arc de Nice

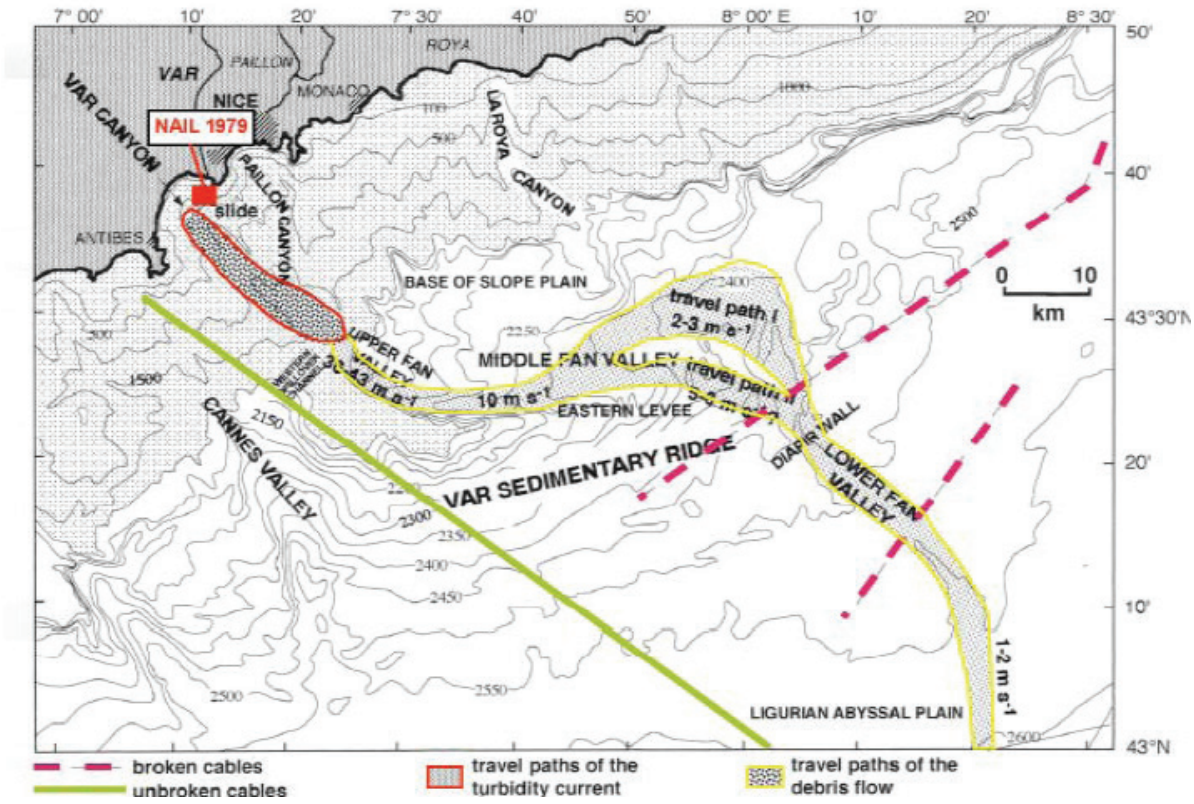

Fig. 1: (continued)

and Arc de Castellane) (Laurent et al. 2000), the closer study area east of 8°E and a few 10s of km south of Nice is seismically characteried by daily microseismicity (Courboulex et al. 2007), abundant small magnitude (M_g = 1.5-3.5) seismic events (several hundreds/yr), and the potential of larger events (M_g = 4.5-5) every 5 years. The largest earthquakes occur offshore, with maximum values of ~M6.5 in 1887 and M6.3 in 1963 in historical times, the former causing >600 casualties, a tsunami, and heavy destruction in several cities along the Ligurian coast (Larroque et al., 2001). Such a large magnitude event may have severe consequences for site-specific ground motion and, thus, sediment failure if close to a city along the French or Italian Riviera (Salichon et al. 2010).

3.1.2 Geological units

The study area is located in the Southern Alps (south-eastern France), in the 25 km long alluvial valley of the Var River. The whole watershed of the Var River is characterised by a large variety of lithologies, not all of which are relevant here (for details refer to Féraud et al. 2009). When looking at the geological maps compiled by BRGM (Fig. 2A) there are four main units which dominate the study area, three of which also govern the aquifer system: (i) the alluvial clastic deposits of Holocene age, (ii) the Pliocene aquifer reservoir (marls and puddingstones), (iii) the „Breche de Carros" consolidated calcareous rocks of

Pliocene or Messinian age (see controversial information in Clauzon [1978] vs. Irr [1984]), and (iv) the aquifer reservoir of Jurassic limestones. At present, water supply in the region comes solely from Quaternary alluvial materials, but studies are underway to secure this resource by tapping into the Pliocene reservoir in the near future (Emily et al. 2010). Given that Potot et al. (2012) found that hardly any GW recharging takes place in the Jurassic limestones, we will focus our attention to the Plio-Quaternary strata. In the lower part of the Var Valley, deposits of the old Var delta fill the Pliocene ria, with two main facies: impervious marls in more distal part of deltaic fan, and about 600m-thick conglomerates (so-called "poudingues du Var", or puddingstones) containing pebbles from rocks outcropping in the whole catchment (see Fig. 2B as an example). The degree of alteration and/or cementation is highly variable in both the marls and puddingstones, with the marls usually appearing to be more heavily weathered. In the alluvial valley, some terraces remain from the Quaternary glaciations and the 100m-thick formation of current alluvia consists of heterogeneous levels of non-consolidated pebbles, sand or marls. In essence, almost all the Holocene material is derived from the Pliocene strata, so that a clear distinction is not always easy. It appears more straightforward in marine seismic reflection profiles, where the top of the so-called „substratum" is characterised by a strong reflection (Savoye & Piper 1991, Kopf et al. 2008; see also Section 2.2 below).

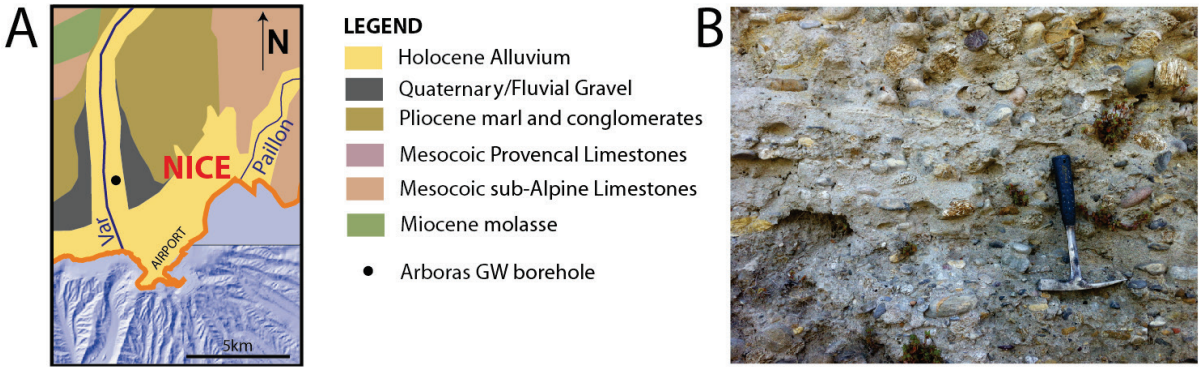

Fig. 2: (A) Geological map of the study area; **(B)** Photograph of Pliocene puddingstones taken near Aspremont during a field trip for preparation of this proposal.

3.1.3 Hydrogeology

The Var system is not only an interesting sedimentological setting, but of major hydrological interest. From a societal point of view, its alluvial aquifer in the lower valley supplies drinking water to more than 600.000 inhabitants of the Côte d'Azur. The Var river is the main source of water for the alluvial aquifer, especially in upstream part. Conglomerate groundwater inputs stand for about 20% of alluvial water recharge (Potot

2011), which is lower than previously estimated. The use of both major and trace elements gives evidences of high heterogeneity in conglomerate groundwater and leads to estimate the proportions of inputs to the alluvial aquifer. Recharge of the alluvial aquifer by Jurassic limestones seems to be insignificant.

When regarding the coastal realm (i.e. the narrow shelf off Nice) as well as the 30-40 km inland, it can first be observed that the entire area reflects the marine post-glacial and Holocene stands. In cross-section, recent deposits are underlain by prodelta and delta sequences, which lie seaward and gently southward-dipping In his PhD thesis, Guglielmi (1993) reported the permeability to be 10^{-3} m/s in the alluvial fluviatiles, 10^{-5} m/s in the delta and prodelta sediments, and 2.6 10^{-6} m/s for the Pliocene substratum. However, these values appear high given that recent reconnaissance measurements on puddingstones ranged between k=7.6 10^{-10} and k=2.8 10^{-11} m/s (Kopf, unpubl. data). Also, a MSc thesis at Univ. Bremen gave a range of k=1.3 – 3.2 10^{-9} m/s for the clayey marine slope apron of Holocene age (Weber 2010). *These variations call for thoroughly revisiting these lithologies over the course of the LISA cruise followed by geotechnical testing at MARUM in order to have solid constraints for hydrogeological models.*

Several researchers have provided evidence for GW seepage in the southern portion of the study transect (i.e. the coastal shelf south of Nice airport). Guglielmi & Prieur (1997) found that lower than average values of some seawater ionic concentrations confirm the existence of freshwater discharge areas. These marine outlets are located where the deltaic impermeable sedimentary cover is thin or even non-existent, and are particularly strong above the 1979 slope failure scar. Gravity cores in that scar revealed strong pore water (PW) freshening (Kopf et al. 2008, 2009), further conforming that some of these waters have strong anomalies in e.g. Cr (most likely contamination from landfilling underneath the airport in the 1960s and 1970s. Repeated visits of the landslide scar by scuba divers revealed that there is often no measurable freshening in the bottom water, even in areas where the gravity cores show freshened PW (Kopf et al., 2009). This implies that submarine GW seepage only occurs during periods of high river discharge from precipitation and snowmelt. Long-term piezometer records from the 1979 scar further attest that the lag time between precipitation and seepage is several weeks to months (Stegmann et al., 2011), although these data are not very robust given that they cover only one full season (see Fig. 3B for details).

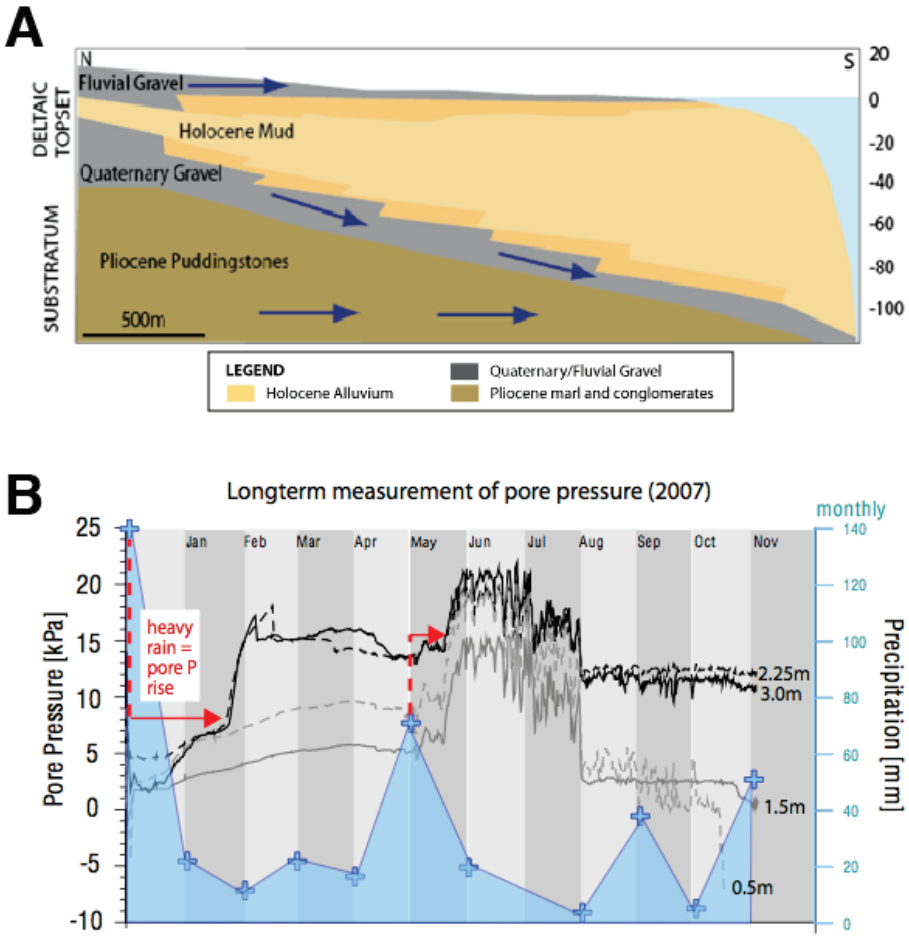

Fig. 3: (A) Cross section modified after Dubar & Anthony (1995) showing the strata in the Nice airport area; **(B)** Long-term record of a piezometer installed in the 1979 landslide scar, showing pore pressure variations at various sub-seafloor levels over time (left y-axis). Also shown is precipitation over the same period (see blue colour and right y-axis). Red arrows mark the delay in response between the rain event and the P record in given sub-seafloor layers.

In a Rn pilot study during cruise Pos386 we used the CEREGE monitoring system from RV Poseidon as well as a dinghy to explore the 1979 landslide scar area as well as the Var river mouth (see Kopf et al. 2009, section 6.3.9 for method, and 7.3.9 for results). We can show that Var discharge water is ageing and degassing and that weak evidence exists for GW seepage in the water column. Tentative estimates suggest a seepage rate of 5mm/day, which is in the same order of magnitude as the estimate by Guglielmi & Prieur (1997). Still, continuous measurements such as those ongoing in the 1979 landslide scar (Stegmann et al., 2012) would be required to monitor the variability as a function of precipitation, snow melt, or other sources.

3.1.4 The 1979 Nice landslide and tsunami

The French and Italian sectors of the Ligurian Margin represent slopes prone to hazardous failure and has collapsed frequently in the past. Risk assessment has hence been a major driver in research concerning the Ligurian slope, in particular after the October 1979

Nice avalanche and associated tsunami, but also because of the frequent flash floods along the French and Italian Rivieras (most recently with 356 mm precipitation in 6 hrs. and massive mudslides; November 2011).

After a period of heavy rainfall, the Nice avalanche occurred on 16 October 1979 on the Var prodelta, causing an embankment of the extended airport construction and underlying sediment to collapse and migrate downslope into the deep Ligurian basin. Based on bathymetry data the volume of failed material was estimated ~0.0022 km^3 near the airport and ~0.0062 km^3 in the mid-slope and displaced sufficient water to generate a tsunami wave of 2-3 m. The resulting debris flow cut two submarine cables (ca. 2400 m and ca. 2600 m water depth; Fig. 1B) some tens of kilometres away from the sliding area, corresponding to progressively decreasing transport velocities from >50 m/s in the steep slope, 36-43 m/s in the Upper fan valley, 10 m/s in the Middle fan valley, and 2-6 m/s when reaching the cables and entering the Lower fan valley towards the deep-sea (Mulder et al. 1997). Parts of the former embankment were transported to > 1000 m depth into the Var canyon. Shortly after the accident, a detailed investigation of the bathymetry was started (Pautot 1981) and several studies aimed to characterize the trigger mechanism(s). An external expert evaluation group (MIP 1981) proposed retrogressive failure, which initiated at the slope and then retrogressively migrated towards the Nice coast and airport. Moreover, the tsunami wave following the slide lowered the sealevel by ~2.5m, which caused static liquefaction of the overloaded slope (e.g. Seed et al. 1988). Also, both the landfill operations preceding the airport extension, where 11 Mill tons of material at water depth of 25m and distances of up to 300m offshore had been additionally put on the slope six month prior to the failure, and heavy rain (250 mm in 4 days) most likely caused considerable overpressure in the delta sequences. Given that both the extra loading and episodic rainfall events (see http://www.hydro.eaudefrance.fr) remain crucial factors destabilising the present-day slope (Dan et al. 2007) identified a combination of creep in the sensitive clay sediments on the Nice slope, loading by landfill material and embankment construction, and pore pressure rise owing to precipitation as main causes for the Nice Avalanche event. This was later confirmed by the monitoring efforts already detailed in the Hydrogeology section above (see also Fig. 3B).

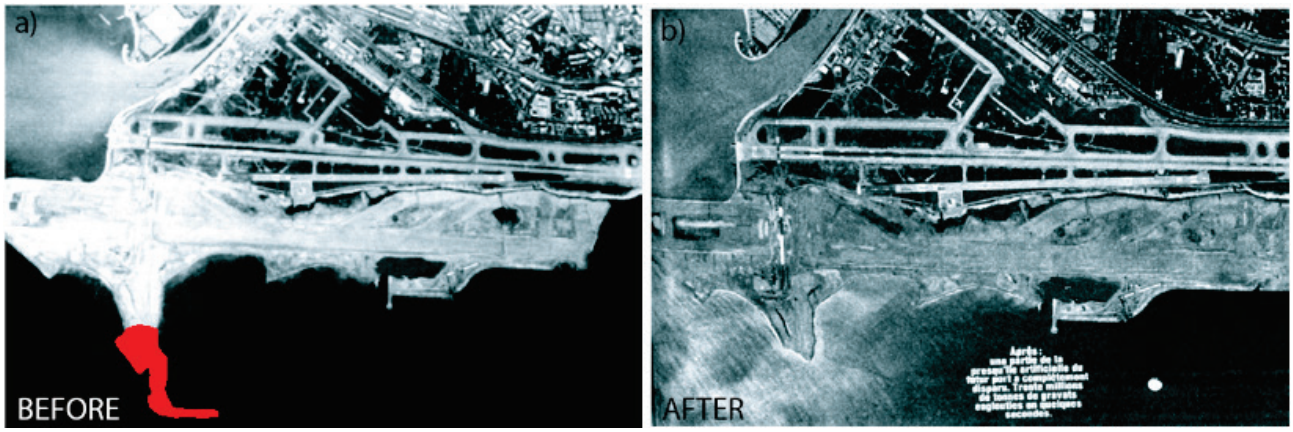

Fig. 4: Aerial photographs of the Nice airport region before and after collapse of the 1979 landslide and destruction of the embankment. From NICE Matin newspaper, 19 Oct. 1979.

Regardless of the exact cause(s) of the 1979 catastrophe, the Nice slope represents one of the few examples on the planet where a suite of different mechanisms that govern slope stability can be studied in an affordable manner (because of the shallow water locality of appx. 30 mbsl). These include, in order of assumed importance:

1. rapid sediment deposition in the Var delta deposits,
2. hydraulic communication between the Var river bed and submarine strata through (presumed) Pliocene substratum and permeable Holocene sand/gravel. The Var river discharge and aquifers charging are cyclic with maxima in November (rainfall) and April-May (rain fall and snowmelt),
3. gently dipping layers of weak sensitive clay, presumably influenced by fluids of reduced salinity migrating in interbedded sand and gravel,
4. seismicity owing to tectonic activity in the Western Alps and the marine realm,
5. additional vertical loading from human land reclaim (e.g. Nice airport peninsula) or construction (harbour embankment) a few decades ago.

In the amphibious drilling and monitoring project by ICDP, IODP and the EU, we will be able to identify and distinguish between the potential triggers of sediment deformation and excess pore pressures unambigously and locate zones of pore water freshening, overpressure, and maximum risk in the future. The proposed *LISA* cruise using RV Poseidon represents a significant milestone towards achieving these goals, most importantly because of (i) an invaluable high-resolution AUV bathymetry to identify regions of incipient sediment deformation and select stable spots for drilling and monitoring, and (ii) to extend the time series data in the 1979 landslide scar observatory (e.g. Stegmann et al., 2012) by continued maintenance and data transfer in 2016.

4. Scientific rationale and State-of-the-art

4.1 Pilot work offshore Nice

For approximately eight years, the PI's working group is concerned with the Ligurian coast and has sailed 7 cruises (chief scientist thrice), worked ionshore, and has led the proposals to IODP, ICDP, and Belmont Forum. Most of this work is published and cited in various places of this proposal, so that we keep the following section brief.

4.1.1 Geophysics

Despite the strict regulations outboard Nice airport we were able to collect pseudo-3D seismic reflection data (see tracks and some examples in Fig. 5). These data served to support the IODP proposal and also put us into a position to estimate the volume of mass wasting in case all sediment above the puddingstones (and not just some underneath the embankment) would collapse in a slope failure event. If the entire shelf region south of the airport collapsed along a detachment of top Pliocene, the volume would be 5-8 times larger than that of the 1979 event. The effects of a subsequent tsunami could be devastating. We use the combined bathymetric information and topographic charts from onshore to do a comprehensive landslide risk assessment study (PhD thesis S. Schnaidt at Univ. Bremen).

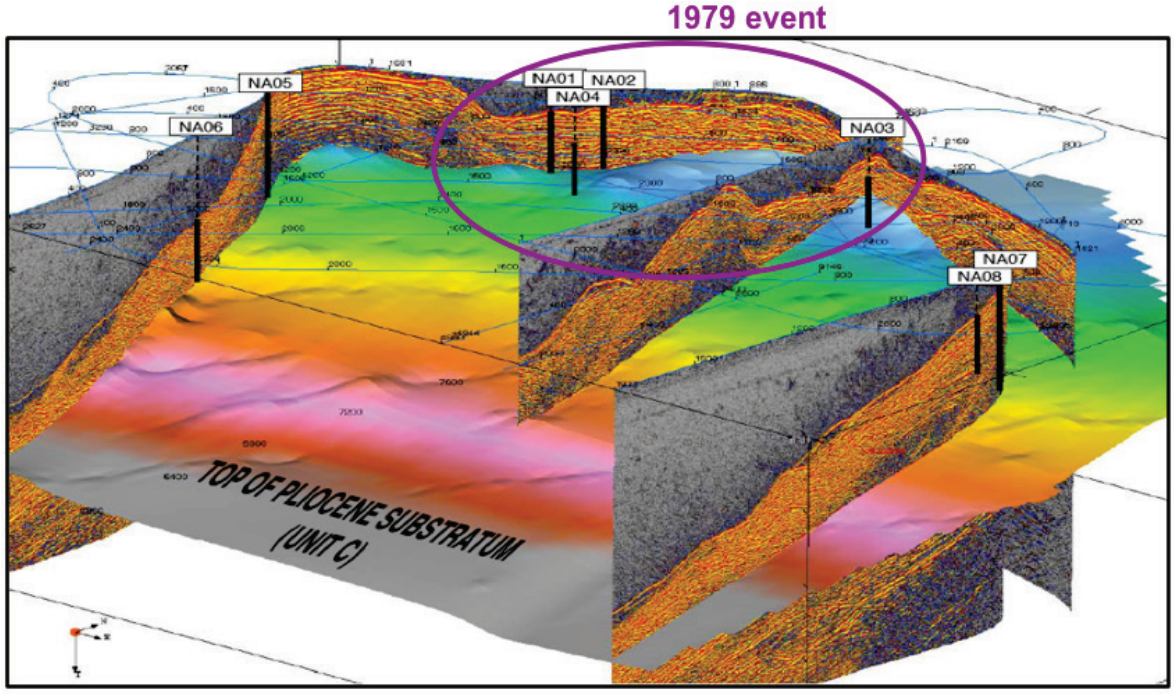

Fig. 5: Geophysical characterisation and proposed IODP drill sites NA1-NA8 (4 primary, 4 alternates). Note that if all material above the puddigstones (projected plane represents top of Pliocene puddingstones) is mobilised, a landslide by far more devastating than the one in 1979 will threaten the French Riviera around Nice.

4.1.2 MAD, Shear strength and Permeability

We routinely carry out moisture & density measurements to get porosity, bulk and grain density, and void ratio of all samples that undergo geotechnical testing (for methodological details, see Blum 1997). In case of the offshore sediments from the Nice slope, this has been published as part of the more detailed papers. Basic shear strength data are obtained on the ship using fall cone penetrometers and vane shear devices (see Kopf et al., 2008, 2009). Ring shear experiments further attested that some of the clay-rich layers are highly sensitive (i.e. large difference between peak and residual strength), most likely as a function of GW leaching (Stegmann et al., 2013). Progressive deformation has also been observed in situ (Penfeld penetrometer) as well as from geophysical acquisition (Sultan et al. 2008, 2010). Regarding permeability testing by our group, see State-of-the-art above and Weber (2010).

4.1.3 Pore water freshening

As stated before, evidence for profound freshening has been provided in various studies. Salinity data from pore water (PW) records are shown in Figure 6, where values drop to literally fresh water concentration regardless of the lithology. Aquifer waters are inferred to migrate fast in the silt, sand and gravel layers while diffusion is hampered by the interbedded clays. Still, hydraulic gradients are rarely sufficient to force the groundwater (GW) into the ocean, but the exact residence time of the fresh PW in the different portions of the transect (onshore, but also offshore) are unknown. The only evidence that exists is from gauges in various parts of the Var valley (see www.eaudefrance.fr for details) which attest that e.g. elevated fluid pressures exist beneath Nice airport (Emily et al. 2010).

Despite these lenses of charged GW, there is also evidence for seawater (SW) intrusion into the landfill materials beneath the airport (Oehler, 2011). There has also been evidence for weakening of clay-rich sediment by leaching ions, as attested by soft sediment deformation, creep, mini-slumps, etc. (Kopf et al., 2016). Continuous monitoring is needed there to e.g. ensure water quality, but also to avoid malfunctioning of air condition systems (Airport authority, pers. comm. 2012).

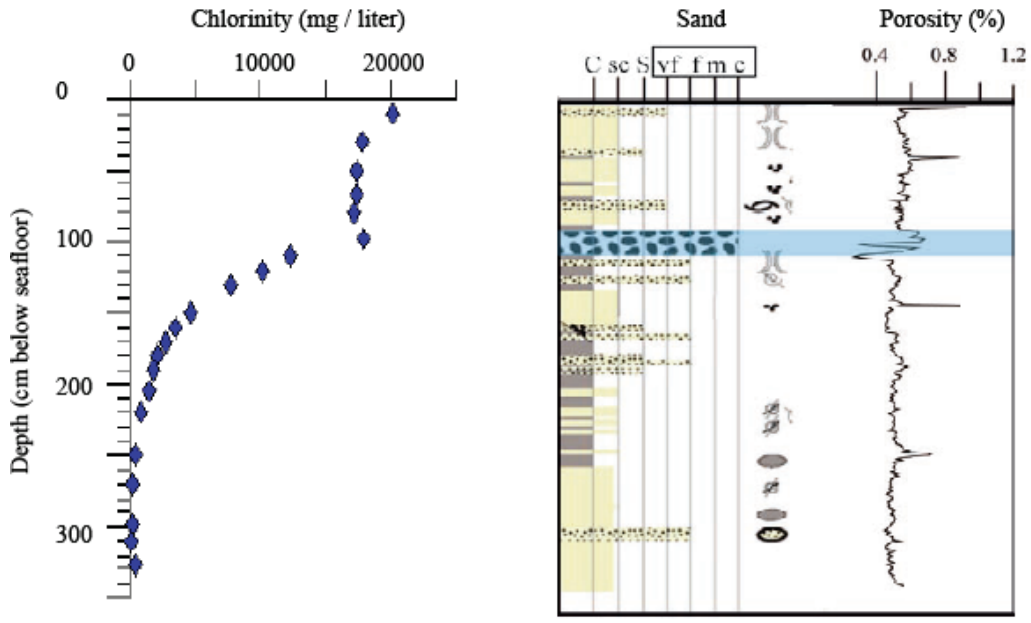

Fig. 6: Lithology, porosity and chlorinity from a gravity core at the headwall of the Nice 1979 landslide (from Oehler 2011).

4.1.4 Excess pore pressure

One key proxy for strain is the transient pore pressure variation in excess of hydrostatic values in a given location and depth. Off Nice, long-term piezometers have been deployed more or less continuously since 2007 in order to assess how pore pressure rises as a function of groundwater charging from precipitation and snow melt as well as sediment deformation (see data examples in Stegmann et al. 2011). We have two piezoprobes plus three other probes deployed as part of a long-term array in the 1979 landslide scar (see Stegmann et al., 2011, 2012), and these systems will be recovered, maintained, and redeployed during the proposed Poseidon cruise.

4.1.5 AUV survey

Earlier work by our French colleagues, in particular cruises MALISAR4 (2009) and AUVNIS (2010) collected EM2000 bathymetry data in a wide area south of Nice, covering parts of the Var and Paillon canyons and the morphologically diverse, landslide prone slope between them (see outline in Fig. 7, and Migeon et al., 2012). Those data helped to identify not only a much laarger number of failure-related scars when compared to studies by Mulder et al. (1996), Klaucke & Cochonat (1999) or Klaucke et al. (2000), but small-scale chute morphologies and other bedforms that hint towards creep processes along the steep (>10° slope angle) portions of the study area (Fig. 7).

During the AUVNIS cruise, the shallowmost portion of the Nice slope were partly mapped, and the portion crucial for our IODP-ICDP approach was part of the area covered (S. Migeon, pers. comm., 2014). With the POS500 AUV data, differential bathymetry research would allow us to identify regions which sport maximum activity and hence represent the highest risk to seafloor installations (e.g. the EMSO hub). At the same time, these regions will be the most promising spots to place sensitive strain meters to monitor incipient deformation processes as precursory phenomena to catastrophic landslides in the future.

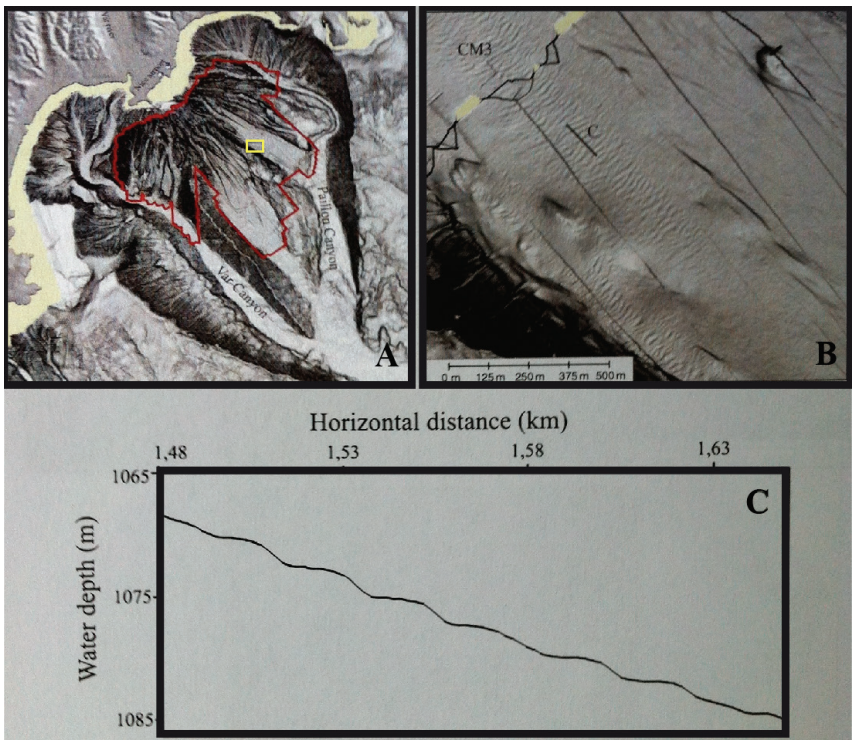

Fig. 7: A) EM300 bathymetry, with the superimposed outline of the AUV EM2000 data. Yellow box shows detailed map in panel B; B) "Chute" pattern on the slope showing both small-scale scars (darker shadows) and wavy, small-scale bedforms that indicate early-stage sediment mobilistion; C) Wavy seafloor pattern with a 20m wavelength and smaller internal features. For location of profile, see panel B. Modified after Migeon et al. (2012).

4.2 Objectives and strategy

4.2.1 Overall objectives of the joint ICDP-IODP-EMSO approach

Given the well-documented history of the 1979 Nice avalance, the wealth of both quasi-static and dynamic/episodic triggers and the large number of subsequent studies, the Nice slope represents an ideal laboratory to identify and quantify physical parameters governing landslide risk unambiguously. The Nice slope has been suspected to be metastable in nature even before 1979 (Dan et al. 2007) so that research efforts in the landslide scar as well as on the stable slopes along strike will solve many of the outstanding

questions concerning the preconditioning factors in slope stability along a glacially overprinted delta system, which is typical for other areas in moderate to high latitudes either side of the Atlantic. The dynamics of the Var system are reflected by tremendous sediment load transported in the river (even more so during periods of snow melt and high precipitation) as well as efficient reworking of the omnipresent Pliocene puddingstones into Holocene coarse-grained deposits.

When revisiting the distinction between long-term governing factors and short-term triggers (Locat 2001; see above), drilling (and coring in particular) serves to get a snapshot concerning the first and a vague idea concerning the latter. In-situ data extends this knowledge towards a more comprehensive understanding on hazard potential and how close to failure a given slope is. Finally, long-term monitoring allows the researcher to monitor transient changes in the properties that govern stability, over long periods of time, but also measure short-term changes and relate them to external forcing (precipitation, earthquakes, human activity, etc.).

As a consequence, state-of-the-art landslide research must try to establish the relationship between the pre-conditioning factors governing an area and the short-term triggers causing a portion of the slope to fail. Offshore Nice, stable shelf areas and recently failed regions occur in close proximity to each other, and to shore. The shallow water depth (largely <50 m) and proximity to a well-developed coastal infrastructure facilitate drilling, in-situ characterisation, and an EMSO cable connections to borehole instrumentation.

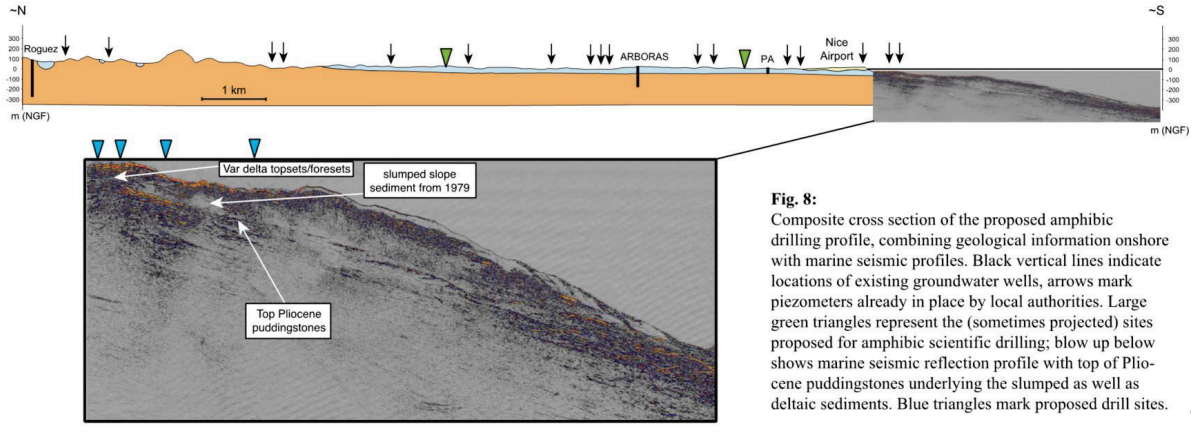

Fig. 8:
Composite cross section of the proposed amphibic drilling profile, combining geological information onshore with marine seismic profiles. Black vertical lines indicate locations of existing groundwater wells, arrows mark piezometers already in place by local authorities. Large green triangles represent the (sometimes projected) sites proposed for amphibic scientific drilling; blow up below shows marine seismic reflection profile with top of Pliocene puddingstones underlying the slumped as well as deltaic sediments. Blue triangles mark proposed drill sites.

In Figure 8 we sketch only the most important sources of information along the transect from the shallow Ligurian Sea onto the continent. From the seismic profile shown as blow-up, the complexity of the shallowmost portion of the shelf and slope-break is evident. This ribbon along the coast is not well represented in the earlier AUV work (see Fig. 7a) and hence requires a detailed investigation and high-resolution mapping. Given the commitment

by EMSO (European Multidisciplinary Seafloor Observatory) to install a shallow-water cable observatory node south of Nice airport in water depth <100 m (S. Garziglia, pers. comm, 2014), a region with minimum disturbance and seafloor deformation has to be identified to not put these future installations at stake.

4.2.2 Main objectives of the proposed expedition

During the proposed cruise *LISA*, we plan the following operations:

(i) recover data from an IFREMER and MARUM piezometers in/adjacent to the 1979 Nice landslide scar,
(ii) recover an osmo-sampler lance adjacent to that location to be able to analyse time-series pore waters geochemically,
(iii) collect additional cores and CPTu in the near the 1979 landslide scar to revisit the issue of active submarine groundwater seepage,
(iv) map the seafloor of the southern end of the amphibious drilling transect proposed to ICDP-IODP to took for the best locations for both drilling and the seafloor cabled node, and
(v) identify areas of sediment creep, incipient slumping, or other evidence of soft sediment deformation that may represent precursors to landslide initiation using processed HR AUV bathymetry.

This proposal follows a coherent strategy of identifying fluids from lateral (onshore portion of the Var aquifer system) and deep sources (diffusive flow from Pliocene puddingstones or silt/sand layers in the delta deposits underlying the slope apron) that favour mechanical weakness by leaching the clay mineral-bearing strata. The anticipated results will complement existing data from earlier cruises (Sultan et al., 2008; Kopf et al., 2008, 2009, 2012) and the aforementioned long-term array in the 1979 scar (Stegmann et al., 2012), and will shed important light on optimising the drilling strategy in an already positively evaluated IODP drilling campaign offshore Nice.

5. Methods

5.1 ELAC MB and AUV bathymetric survey with MARUM SEAL 5000

5.1.1 ELAC Multibeam system

During cruise POS500, the multibeam sonar system *Multibeam 3050* from *L-3 Communications ELAC Nautik* was used. To determine the structure and depth of the sea floor, a short pulse of sound (ping) is generated by a projector. The created signal travels as compressional wave through the water. The local speed of sound depends on salinity, pressure and temperature. As the wave front is interrupted by the sea bottom, a certain factor of the energy is reflected. This reflected signal (echo) has the same frequency than the source wave and is recorded by hydrophones which measure the oscillations in pressure as the pressure front of a sound wave passes. Knowing the travel time and the speed of the sound in water the depth of the sea bottom can be calculated.
A multibeam sonar allows to map more than one location of the sea floor with one single ping. The bottom locations are arranged to map a contiguous strip perpendicular to the path of the survey vessel. The dimension of this stripe is the swath width. The advantage of a multibeam system in comparison to a singlebeam system is a higher survey speed.

In order to determine the exact position of the echoes occurring along the ship, the projector and hydrophone array are installed perpendicular to each other (Mills cross arrangement). Using this arrangement, the area of the ocean floor ensonified by the projectors intersects with the area observed by the hydrophones only in a small area. The dimensions of this area correspond approximately to the projector and hydrophone array beam widths.
The range of the instrument is limited by the amount of attenuation and by the noise level. Errors that would occur due to yaw and pitch motion of the vessel are fully compensated by a transmit technique of the *Seabeam 3050* by splitting the transmitted fan in several sections which can be steered individually.

The *Multibeam SB 3050* system on *Poseidon* is designed to operate in depths from 3 m to approximately 3000 m. The operating frequency is in the 50 kHz band. Maximum ping rate is 50 swaths per second and the maximum number of beams is 315. The maximum across-ship swath coverage sector is 140 degrees.

The hardware components of the *Seabeam 3050* system include a motion sensor, a positioning system, a sound velocity profiler and a surface sound velocity sensor. An

operating computer receives the preprocessed data stream. Bathymetric data can be visualised in real time using the *Hypack* (2) mapping tool. A schematic diagram of these different components can be seen in Figure 9.

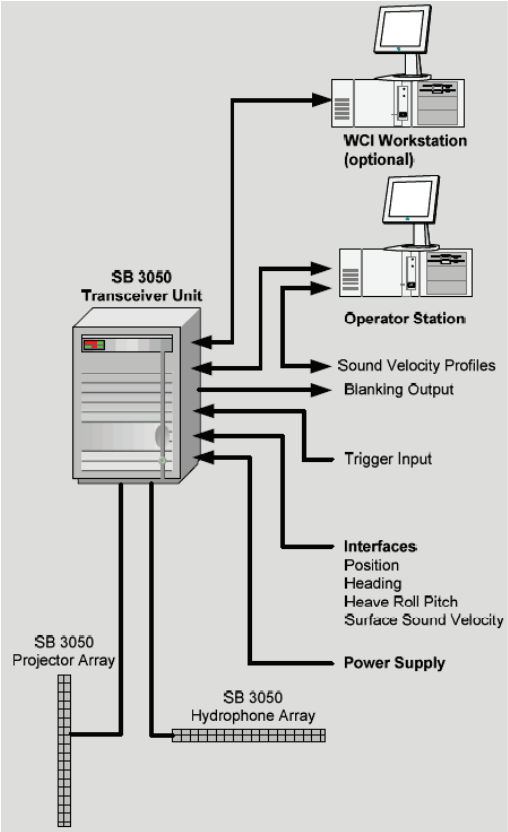

Fig. 9: Layout of the Multibeam system recently installed on RV *Poseidon*. See text.

5.1.2 AUV bathymetric survey with MARUM *SEAL 5000*

Introduction

In the year 2006 the MARUM ordered a deep diving autonomous underwater vehicle (AUV), designed as a modular sensor carrier platform for autonomous underwater applications. The company International Submarine Engineering (I.S.E.) built this AUV in Canada. In June 2007 the AUV "SEAL" was delivered to MARUM and tested afterwards on the French vessel N/O SUROIT (June 2007) and the German R/V POSEIDON (November 2007) in the Mediterranean Sea. Since then, the AUV is in operational mode and was used 12 times before on field cruises on-board research vessels (R/V SONNE, R/V METEOR, R/V M.S.MERIAN, R/V POSEIDON, N/O SUROIT, R/V OR5) and 2 times in Lake studies (Lake Constance, Lake Neuchatel). Therefore, this R/V Poseidon cruise POS500 is the 13th field cruise of MARUM SEAL.

SEAL vehicle – Basics

The MARUM AUV Seal is No. 5 of the Explorer-AUV series from the company I.S.E. (see Fig. 10). The AUV is nearly 5.75 m long, with 0.73 m diameter and a weight of 1.35 tons. The AUV consist of a modular atmospheric pressure hull, designed from 2 hull segments and a front and aft dome. Inside the pressure hull, the vehicle control computer (VCC), the payload control computer (PCC), 8 lithium batteries and spare room for additional "dry" payload electronics are located. Actually, the inertial navigation system PHINS and the RESON multibeam-processor are located as dry payload here. The tail and the front section, build on GRP-material, are flooded wet bays. In the tail section the motor, beacons for USBL, RF-radio, Flashlight, IRIDIUM antenna and DGPS antenna are located. In the newly constructed aluminium front section the Seabird SBE 49 CTD, the Sercel MATS 200 acoustic modem, the DVL (300kHz), KONGSBERG Pencil beam (675kHz), the recently implemented KONGSBERG EM2040 (200,300, 400kHz), the PAROSCIENTIFIC pressure-sensor and the BENTHOS dual frequency (100/400kHz) side scan sonar are located (optional). Actually, the SEAL AUV has a capacity of approx. 15,4 KWh main energy, which enables the AUV for approx. 65 km mission-track lengths, which has to be reduced due to the more energy consuming EM2040 MBES compared to former cruises.
For security aspects, several hard- and software-mechanisms are installed on the AUV to minimize the risk for malfunction, damage and total loss. More basic features are dealing with fault response tables, up to an emergency drop weight, either released by user or completely independent by AUV time-relays itself.

MARUM put special emphasise on open architecture in hard- and software design of the AUV, in order to be as much as possible modular and flexible regarding the vehicle operations. Therefore, the VCC is based to large extend on industrial electronic components and compact-PCI industrial boards and only very rare proprietary hardware boards have been implemented. The software is completely built QNX 4.25 – a licensed UNIX derivate, to large extends open for user modifications. The payload PC is built on comparable hardware components, but running either with Windows and/or Linux.

On the support vessel, the counterpart to the VCC is located on the surface control computer (SCC). It is designed as an Intel based standard PC, also running with same QNX OS and a Graphic User Interface (GUI) to control and command the MARUM SEAL AUV. Direct communication with the AUV is established via an Ethernet-LAN, either by hard-wired

100mb LAN cable plugged to AUV on deck, or by Ethernet-RF-LAN modem - once vehicle is on water. The typical range of RF-communication is around 1 – 2 km distance to vehicle.

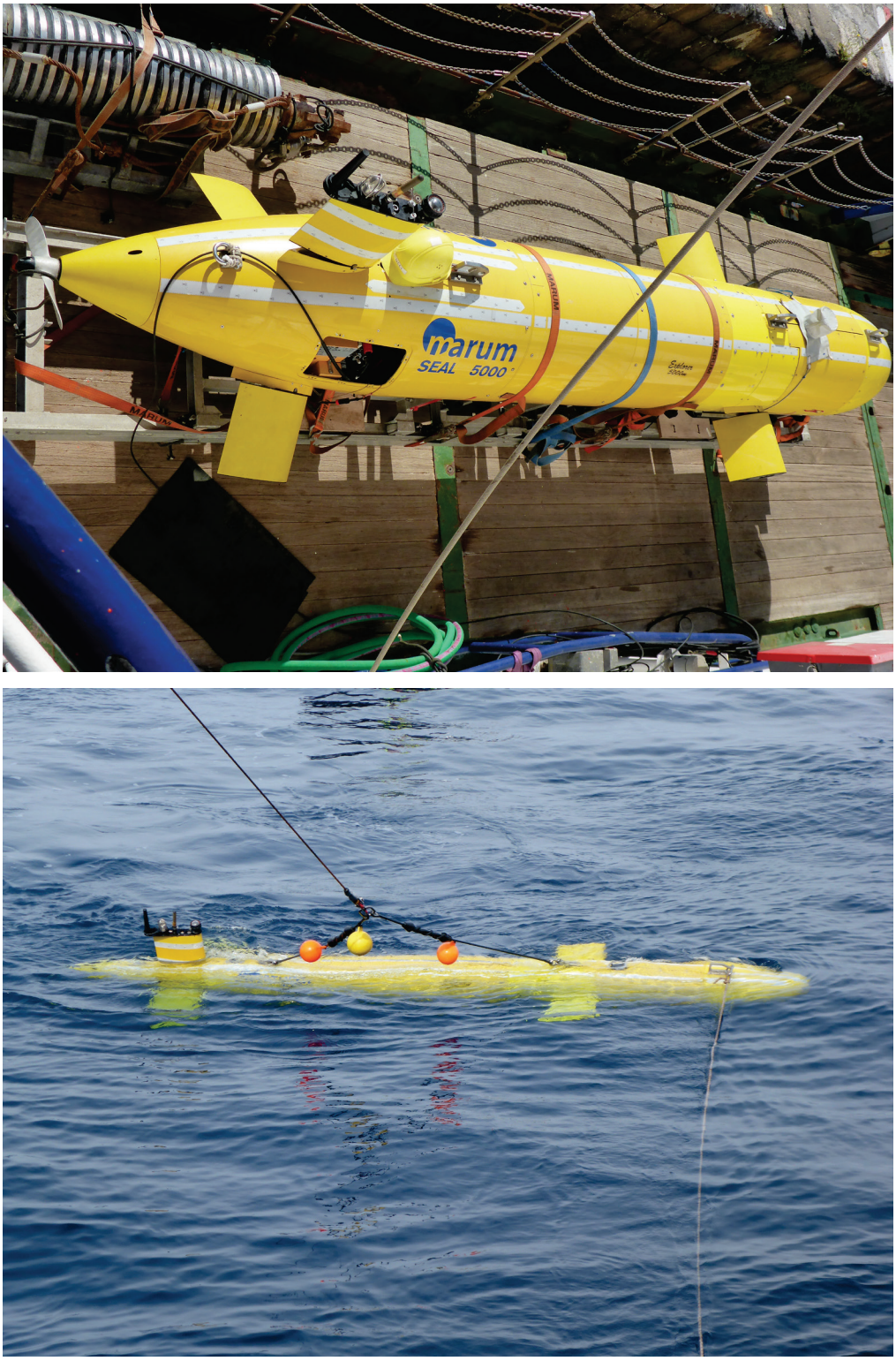

Fig. 10: AUV SEAL on deck of RV Poseidon (previous page) and when launched for one of the missions off Nice, France (above).

Within this range the user has all options to operate the AUV in Pilot-Mode, e.g. to manoeuvre the AUV on water or change vehicle settings. Once the AUV is under water, all communication links were shut down automatically and the AUV has to be in Mission-Mode, means it is working based on specific user-defined missions.

Despite being in mission-mode it is necessary to communicate with the AUV when it's under water, i.e. asking for actual position, depth and status. To achieve this, on-board the support vessel an acoustic underwater modem with dunking transducer has to be installed (SERCEL MATS modem) communicating with the counterpart on the AUV, on request. Due to limited acoustic bandwidth only rare data sets are available.

Mission-Mode

The AUV - as dedicated autonomous vehicle - has to be pre-defined operated under water, by demand. As mentioned, only at sea surface a manoeuvring by the pilot is possible - once it dives, it will looses communication and therefore must be in a mission-mode. Initialized correctly, fault prevention mechanisms should prevent the AUV for damage/loss in that case.

Simplified, an AUV mission is a set of targets; clearly defined by its Longitude, Latitude, and a given depth/altitude the vehicle should reach/keep by a given speed of AUV in a distinct time. The AUV needs to be in a definite 3-dimensional underwater space to know exactly its own position over mission time in order to actively navigating on this. To achieve this basic scenario, the AUV is working at sea surface with best position update possible, e.g. DGPS position. Once it dives, it takes the actual position as starting point of navigation, looks for its own heading and the actual speed and calculating its on-going position change based on the last actual position, e.g. method known as dead reckoning. To achieve highest precision in navigation, a combination of motion reference unit (MRU) and Inertial Navigation System (INS) is installed on the MARUM SEAL AUV – the PHINS inertial unit from IXSEA Company. Briefly, the MRU is "feeling" the acceleration of the vehicle in all 3 axis (x,y,z). The INS is built on 3 fibre-optic gyro's (x,y,z) and gives a very precise/stable heading, pitch and roll information, based on rotation-changes compared to the axis. Even on long duration missions, the position calculating by the AUV will be very accurate based on that technique.

Mission planning

In principle and very briefly, it would be accepted by the vehicles VCC to receive a simple list of waypoints as targets for the actual mission (the list has to be in a specific syntax). In order to arrange it more efficient and convenient a graphical planning tool is used for this mission planning. The MIMOSA (© Ifremer) mission-planning tool is a software package specially designed to operate underwater vehicles (AUVs, ROVs, Glider). The main goal of this software is to plan the current mission, observe to AUV once it is underwater and to visualize gathered data from several data sources and vehicles.

MIMOSA is mainly built on 2 software source, e.g. an ArcView 9.1 based Graphical Information System (© ESRI ArcGIS) and professional Navigation Charting Software (© Chersoft UK).

In order to plan a mission the user has to work on geo-referenced charts with a given projection (MERCATOR); either GIS-maps, raster-charts or S-57 commercial electronic navigational charts (ENCs). These basic charts could enlarged easily with user specified GIS projects, enhanced with already gathered data, e.g. multibeam data, point of interests. Once installed in MIMOSA, one can create AUV missions by drawing the specific mission by mouse or using implemented set of tools (MIMOSA planning mode). Missions created in that way are completely editable, movable to other geographical locations and exportable to other formats. In order to be interpretable by the MARUM SEAL AUV, the created mission will be translated in the I.S.E. specific syntax; a set of targets, waypoints, depths information and timer will be created and written into an export path. From here the mission file can be uploaded via the SCC (support vessel) into the VCC (AUVs control PC); the AUV has its mission and is capable to dive, based on a valid mission plan.

Mission observing/tracking

The MIMOSA planning tool is also used for supervision, e.g. to monitor the vehicle at sea surface and more interesting under water (MIMOSA observation mode). The MIMOSA software is client based, means one dedicated server is used for planning, while the others are in slave/client mode, picking up actual missions. Therefore, position data strings (UDP broadcast data) from the support ship (i.e. R/V Poseidon / position, heading) are being sent to local network and fed into the MIMOSA software; the same is active for the AUV

position data, e.g. DGPS signal once it is on sea surface. During dive the AUV can be tracked automatically via ship-borne ultra short baseline systems (USBL), e.g. IXSEA GAPS or POSIDONIA, using the on-board AUV installed USBL transponder beacon responded signal (delivers position where the vehicle "actually" is).
In addition to this independent position source, vehicles own position (deliver where the vehicle "thinks" it is) can be displayed also. This position is based on transmitted data strings from MATS underwater acoustic modem, only sent from AUV on user request.
To summarize, usually you have displayed in tracking mode:

- position of support vessel (lon/lat and heading)
- either DGPS of AUV during surface track, or
- USBL position (GAPS or POSIDONIA)
- and MATS position (underwater acoustic on request)

Operational aspects

In general, MARUM SEAL was used at least 13 times on field cruises so far. Thus, several different vessels have been in operation and on each vessel the handling of the AUV is quite a bit different. In principle, the A-frame seems to be the best position to launch and recovery the AUV, because the tendency to hit ships wall is minimized compared to sideward operation, based on experiences. On R/V Poseidon 500 the AUV was operated successfully with the main ship crane at portside of vessel, which works very well.

In principle, the AUV can be operated out of the lab, just with simple PC-console racks. On R/V Poseidon 499 cruise, the AUV operations were run out of a 20" operation/workshop van, located on the main deck, aft. The consoles, file-server and printer are installed in the container, workbench, tools and spares as well. The SERCEL MATS acoustic transducer was installed into the moon pool from R/V Poseidon. For USBL positioning, the IXBLUE GAPS system was used, installed in the moon-pool as well.

Prior to launch of AUV, the PHINS INS (on-board the AUV) needs to be calibrated (as well as the GAPS system). Therefore, it has to be reset and the support vessel has to be still standing for at least 5 minutes. After that initial phase (INS coarse align), the vessel needs to run a rectangular course; square-coarse, 5 minutes @ 3-5 knots each line (INS fine align). At the end of that time-span and course, the PHINS is in so called "normal mode", means it has its highest position quality.

5.2 Gravity & push coring and sediment description

5.2.1 Coring techniques

In order to recover sediment cores, two sampling systems were used during POS500: (i) a gravity corer with tube lengths of 3 to 6 m and a weight of approximately 2 tons (Fig. 11), and (ii) a light-weight "mini corer" of only 100 cm length for use in very shallow water and sampling of the mudline and uppermost sub-seafloor (Fig. 12). Before using the gravity corer, the plastic liners that are placed inside the steel tubes were marked lengthwise with a straight line in order to retain the orientation of the core for paleomagnetic analyses.

Fig. 11: Gravity corer on board R/V *Poseidon*.

Once on board, the sediment cores were cut into sections of 1 m length, closed with caps on both ends and labelled according to a standard scheme (Fig. 13). For the time being all cores were preserved as whole rounds for future geotechnical experiments.

The MIC cores were not preserved intact, but were transferred into a plastic bag. A water sample of the bottom water (above the core) as well as an interstitial fluid sample taken by rhizon (see geochemistry section below) from the bagged sample were extracted before the push corer was cleaned again for the next deployment.

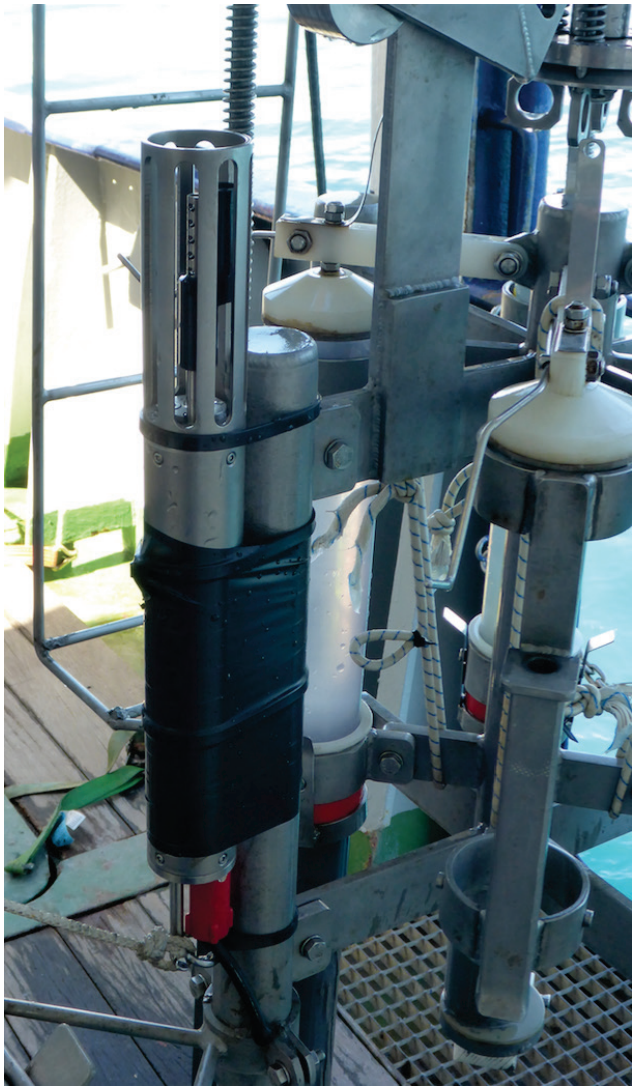

Fig. 12: Mini pushcorer (also short MIC) with CTD mounted (left) on board R/V *Poseidon*.

5.2.2 Sediment characterisation

Gravity cores of this expedition were not split and lithologically described, but (i) first used to extract pore water for salinity study to assess groundwater influence, and (ii) second run through a GEOTEK MSCL (multi sensor core logger), a device that combines three sensors on an automated track (see schematic diagram in Fig. 14). The P-wave velocity, gamma ray attenuation (bulk density), and the magnetic susceptibility were recorded, and from this data the fractional porosity and impedance were calculated. The line scan camera was not used since it is restricted to split cores, however, all POS500 cores are preserved for future geotechnical experiments using whole round samples.

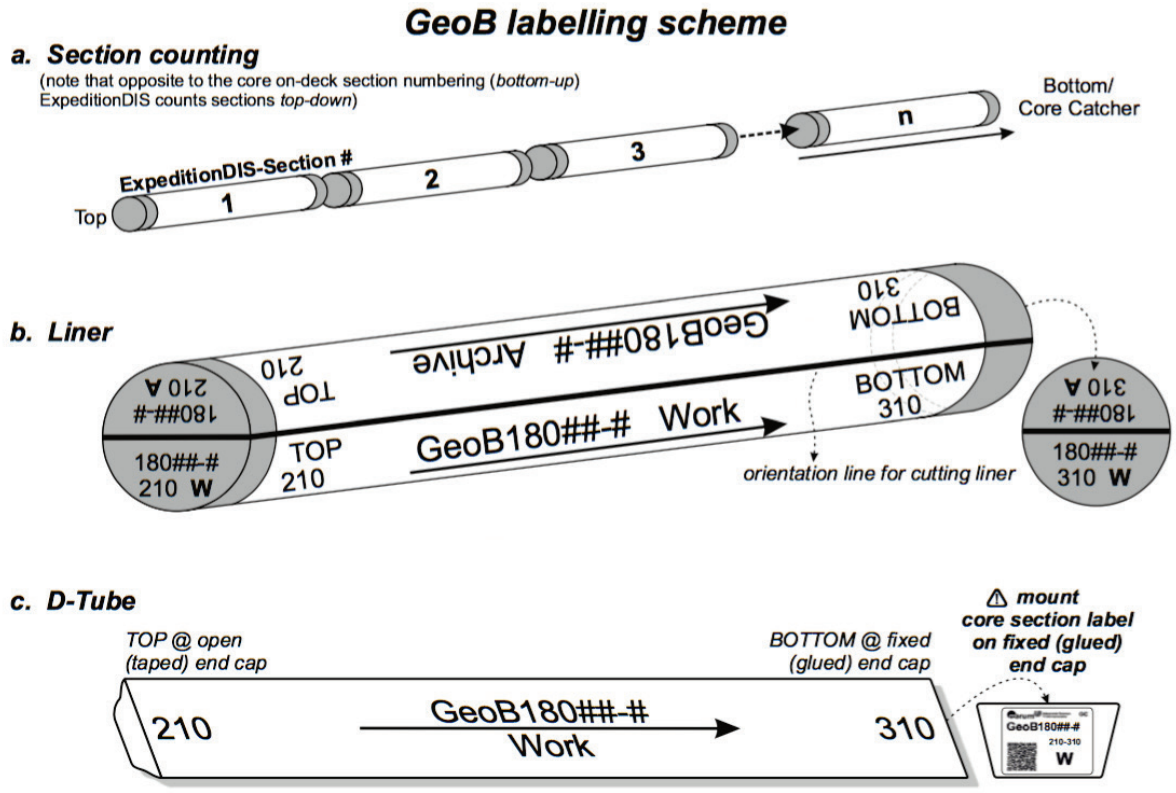

Fig. 13: Scheme of the inscription of gravity core segments used during POS500 (GeoB215##-#).

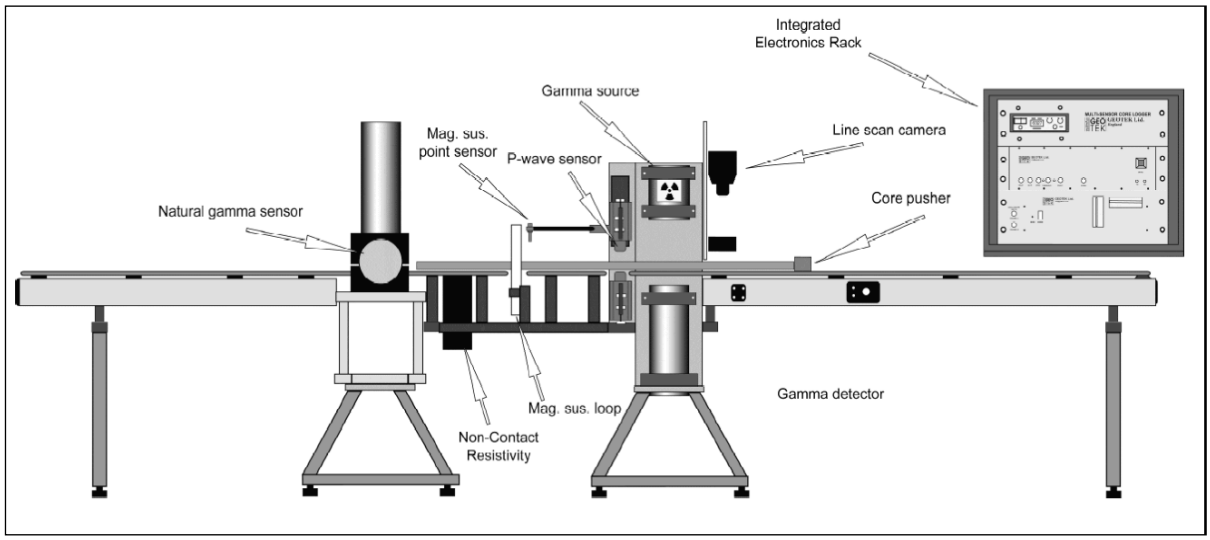

Fig. 14: Schematic drawing of the Geotek Multi Sensor Core Logger (MSCL).

5.3 CTD and bottom water sampling

Apart from the CTD moounted to the push coring device (see above), we also included a CTD (Sea & Sun Technologies) into the frame with the Niskin bottle for bottom water sampling. The device is shown in Figure 15 and illustrates the lower portion with Niskin bottle and its release (i.e. 3 POM disks mounted on springs) and the CTD above it.

The instrument mainly focused on sampling the bottom water in regions suspected of submarine GW seepage. The added bonus is that the CTD records how salinity changes vertically across the water column.

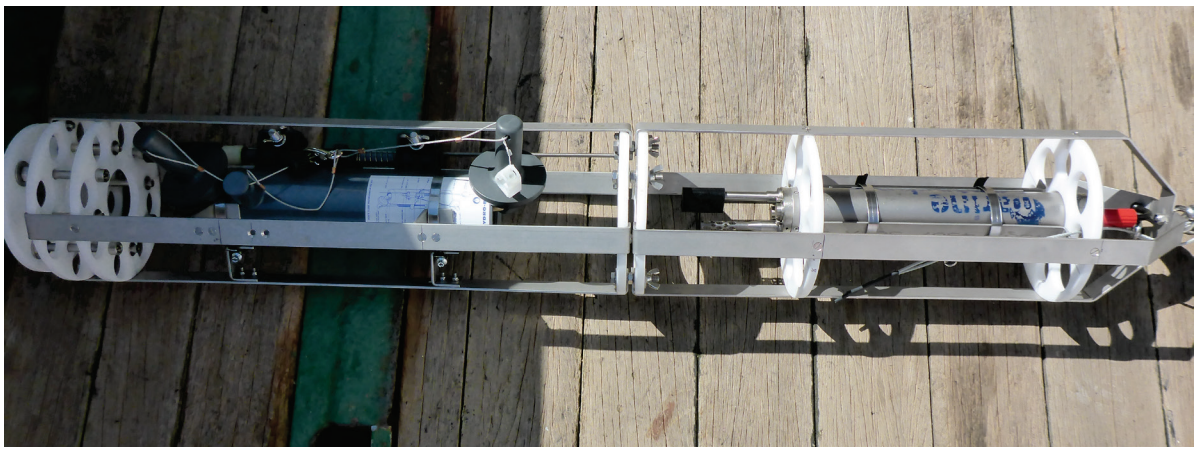

Fig. 15: Bottom water sampler with 1l Niskin bottle and CTD mounted at the top (right). See text.

5.4 Pore water chemistry

All gravity cores were taken by plastic liners and cut into 1 m segments on deck. To prevent a warming of the sediments on board, the sediment cores were immediately transferred into the cooling room after recovery and maintained at a temperature of about 4°C. The wet sediment was exposed by means of cutting a small 'window' in the plastic liner at an interval of 25 cm. Salinity was measured directly using a hand-held refractometer (Fig. 16A). The pore water was then extracted by means of rhizons (pore size 0.1 µm) (see Fig. 16B). The gravity cores were each processed in this way within a few hours after recovery. Depending on the porosity of the sediments, the amount of pore water recovered ranged between 1 and 10 ml. Solid phase samples of the majority of cores were taken for total digestions, sequential extractions and mineralogical analyses at 25 cm intervals, kept in gas-tight glass- and heavy plastic bottles under an argon atmosphere and stored at 4°C.

For the MIC push cores, we had to transfer the sediment into a plastic bag as soon as the corer was back on deck. For each core recovered, we hence took a bottom water sample above the mudline and then used the rhizons to extract interstitial waters from the sediment.

Pore water analyses of the following parameters were deferred to the shore-based laboratories at Bremen University. The only quick measurement on board was salinity using a refractometer.

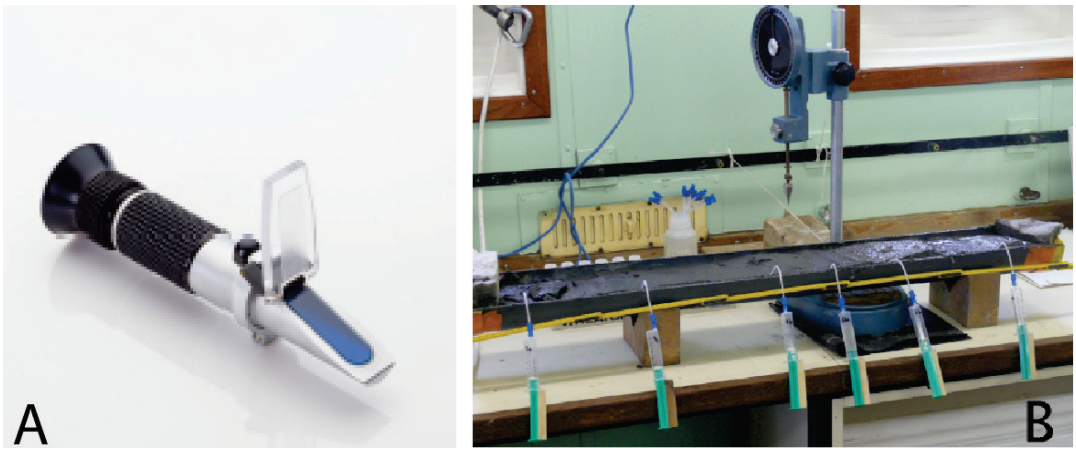

Fig. 16: (a) Hand-held refractometer for salinity estimate, and (b) rhizon pore water extraction in split working half of the gravity core.

For further analyses at the University of Bremen aliquots of the remaining (pore) water samples were diluted 1:10 and acidified with ultra pure HNO_3 for determination of cations (Ca, Mg, Sr, K, Ba, S, Mn, Si, B, Li) by ICP-OES. Additionally, 0.6 mL of a ZnAc solution was added to a 1.5 mL subsamples of the pore to fix hydrogen sulfide as ZnS for later analysis. Finally, all remaining pore water was stored at 4 °C for additional analyses at the University of Bremen. A complete overview of sampling procedures and analytical techniques used on board and in the laboratories at the University of Bremen is available on http://www.geochemie.uni-bremen.de/.

5.5 MCS reflection survey

The GeoB multichannel seismic equipment is designed to collect high-resolution seismic data using different acoustic sources, multichannel streamers partly equipped with a bird controller system, the custom-designed acquisition system MaMuCS and a trigger system. In the following, all components are described in detail.

During Cruise POS500 a Sodera micro GI-Gun with 2 x 0.125 L volume (frequency range between 100 and 800 Hz). The micro GI Gun was towed on the starbord side using the standard hanger assembly appx. 15 m behind the stern. Towing geometries are shown in Figure 17. The source was shot at 3 sec shot intervals with an average pressure of 100 bar. The air was provided by a compressor on the deck of RV Poseidon. The air was stored in a bottle battery from where it was supplied to the GI-Gun via an umbilical.

For acquisition of the seismic data a conventional analogue streamer (Teledyne) was towed on the port side of the ship. It contains 64 hydrophones with a spacing of 1 m for the first 32 channels and 4 m for the last 32 channels, providing a total length of the active section of 160 m. Separating the active section from the ship was a stretch section of 10 m length and a lead-in of about 15 m length.

The streamer was kept at a towing depth of 1 m with the help of 4 Digicourse Birds. Due to damage to one of the birds during the first day of surveying, only 3 Birds were used for streamer depth control from June 3rd onwards. Bird depths were set before and during the surveys through the Digi Bird Controller.

For data recording of the 16 channel analog streamer, the custom-designed and PC-based 96-channel seismograph Marine MultiChannel Seismics (MaMuCS) was used. It is based on a Pentium IV PC (3 GHz, 2 GB RAM) with Windows XP operating system and was operated at a sampling rate of 0.125 ms at 16 bit resolution with a recording length of 1.5 seconds. It is equipped with three 32-channel multiplexers (NI 1102C) and three A-D converters (NI 6052E) of which only two sets were used due to the streamer only having 64 hydrophones. The seismograph provides online data display of shot gathers as well as a brute stack section of the range of channels of the user's choice, and stores data in SEG-Y format on the internal hard disk drive. First back-up copies were created during intervals of no seismic activity on an external disk. Anti-aliasing filters were fixed to 10 kHz on the AD converter. Gain for each channel was set to 100 (measurement range 0.1 V).

The trigger unit controls the timing of seismic sources, the recording units, and the bird controller. The custom made 6 channel trigger generator (SCHWABOX) was used in conjunction with a two channel trigger amplifier driving the solenoid valves of the GI Gun. The SCHWABOX is connected via USB to the Trigger-PC and programmed with a small custom software tool. The system allows defining arbitrary combinations of trigger signals. Trigger times can be changed at any time during the survey. Through this feature, the

recording delay can be adjusted to any water depth without interruption of data acquisition. Due to the very shallow water depths, the seismic source as well as the recording of the data were started simultaneously.

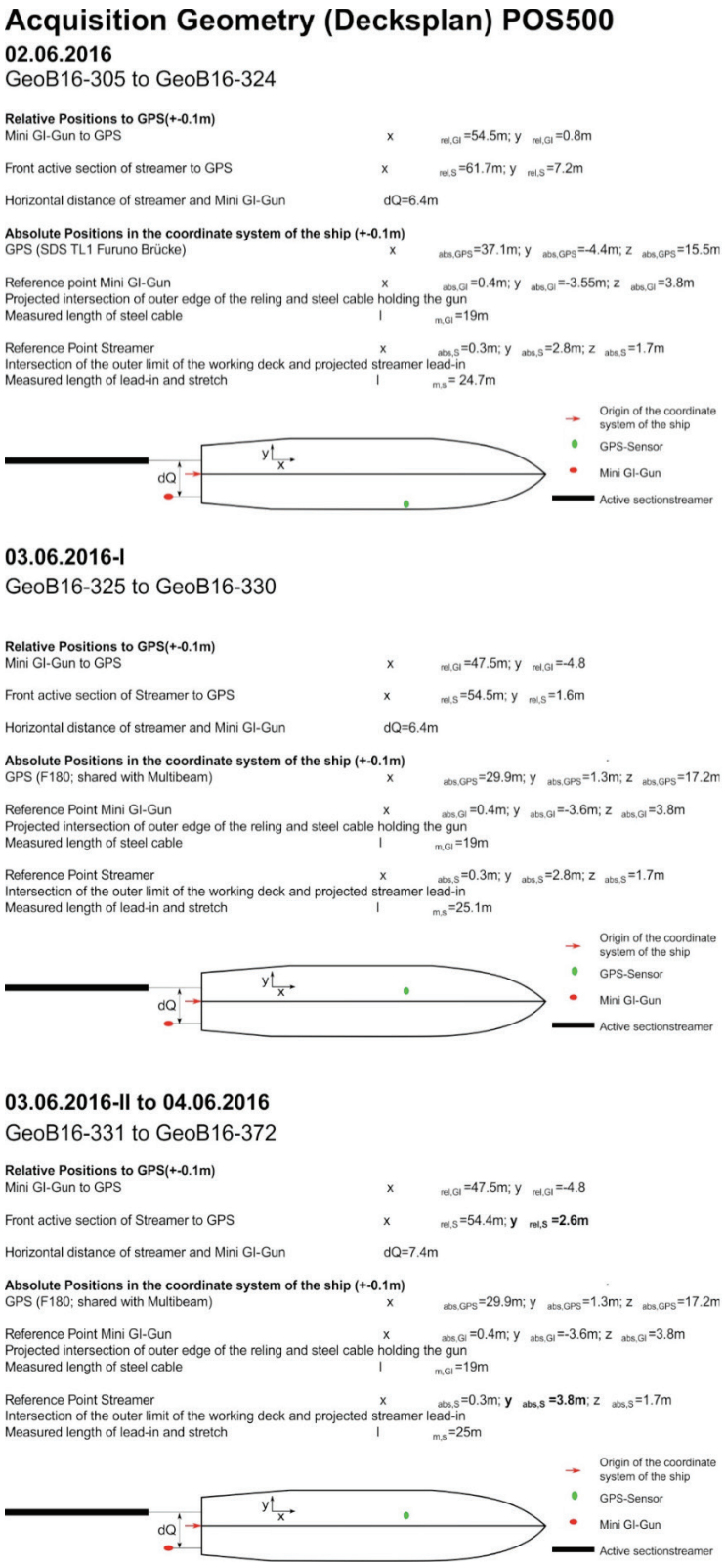

Fig. 17: Towing geometry of the multichannel seismic system

5.6 Long-term observatory tests

5.6.1 MeBoPUPPI

For the MARUM seafloor drill rig MeBo (Freudenthal & Wefer, 2013), the Marine Geotechnics working group has developed a series of borehole observatories. Three different systems have been developed for the MARUM-MeBo (Meeresboden Bohrgerät) seafloor drill, which is operated by MARUM, University of Bremen, Germany. A simple design, the MeBoPLUG, separates the inner borehole from the overlying ocean by using o-ring seals at the conical threads of the drill pipe. The systems are self-contained and include data loggers, batteries, thermistors and a differential pressure sensor.

A second design, the so-called MeBoCORK (Circulation Obviation Retrofit Kit), is more sophisticated and also hosts an acoustic modem for data transfer and, if desired, fluid sampling capability using osmotic pumps. Of these MeBoCORKs, two systems have to be distinguished: The CORK-A (A = autonomous) can be installed by the MeBo alone and monitors pressure and temperature inside and above the borehole (the latter for reference). The CORK-B (B = bottom) has a higher payload and can additionally be equipped with geochemical, biological or other physical components. Owing to its larger size, it is installed by ROV and utilises a hotstab connection in the upper portion of the drill string. Either design relies on a hotstab connection from beneath which coiled tubing with a conical drop weight is lowered to couple to the formation. These tubes are fluid-saturated and either serve to transmit pore pressure signals or collect pore water in the osmo-sampler.The details can be found in Kopf et al. (2015).

In a recent effort, we have taken the MeBo long-term borehole observatory science to the next level and build pop-up borehole instruments that can be released from the casing string after a predefined period. An underwater mateable connector further enables the user to also „manually" release the unit by ROV. Once the unit has ascended to sea level, the popup unit (Fig. 18) send their data via satellite link, rendering a second visit and additional shiptime unnecessary. Such instruments would in a first iteration monitor pressure and temperature, but could be equipped with geophones, seismometers and other components depending on the scientific demands of a given mission, the duration of monitoring, the amount of time series data, etc..

As seen in Figure 18, the MeBoPUPPIs monitors pressure and temperature inside and outside of the borehole as well as tilt using a triaxial array of accelerometers. If desired, an

additional unit that samples simultaneously one hydrophone and three geophone channels (type SM6, with 4.5 Hz lower frequency band, but no mechanical gimbaling system) can be mounted. Either sensing package has to remain in the borehole string for reasons of limited space and weight of the popup unit. This may be equally the case for part of the battery packs when very long monitoring periods are desired.

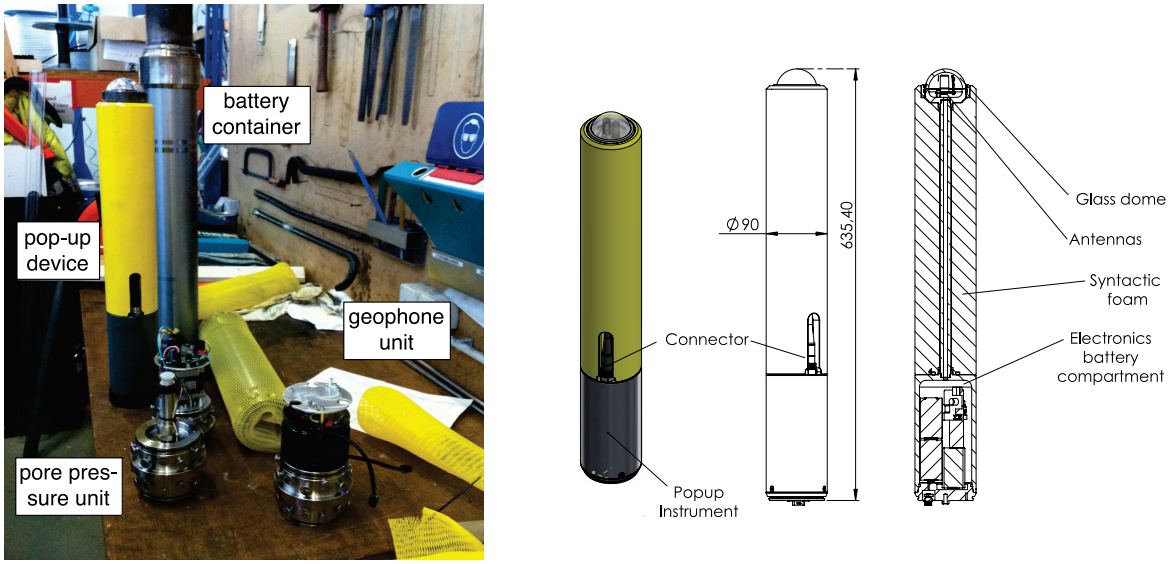

Fig. 18: Schematic diagram (right) and photograph (left) of MeBoPUPPI observatory.

In contrast to the MeBoCORK systems, the MeBoPUPPIs do not rely on a hotstab connector and tubing that is lowered towards terminal depth of the borehole where direct access to the formation exists. Instead, the monitoring is restricted to pressure and temperature inside and outside of the borehole as well as tilt using a triaxial array of accelerometers. If desired, an additional unit that samples simultaneously one hydrophone and three geophone channels (type SM6, with 4.5 Hz lower frequency band, but no mechanical gimbaling system) can be mounted. Either sensing package has to remain in the borehole string for reasons of limited space and weight of the popup unit. This may be equally the case for part of the battery packs when very long monitoring periods are desired. In these cases, almost all of the total of 235 cm length of a MeBo70 drill rod segment, excluding a 53 cm-long adapter to protect the glass dome (Fig. 18, righthand side drawing) are available.

For the long-term test in the Nice 1979 landslide scar, the instrumented MeBoPUPPI drilling rod was modified in a way that enables the user to run it as a piezometer probe using a weight stack with release for deployment. We hence built an adapter that reduces the diameter of the lower part of the probe from ~10 cm to half that value along a 1,4 m-long

metal rod with conical tip. The tip has a porous stone that protects pore pressure tubing that runs from the tip to the pressure transducer in the upper (observatory) part of the device.

Figure 19 shows the assembled observatory on deck of RV *L'Europe*. Given the test scenario, part of the disposable observatory were covered in shrink wrap to minimise corrosion. The configuration used includes pore P, T, tilt and seismicity. The instrument was then clamped into a base plate that is compatible with the IFREMER weight stack. The latter was used with an acoustic release in order to deploy the instrument in the 1979 landslide scar (Fig. 19).

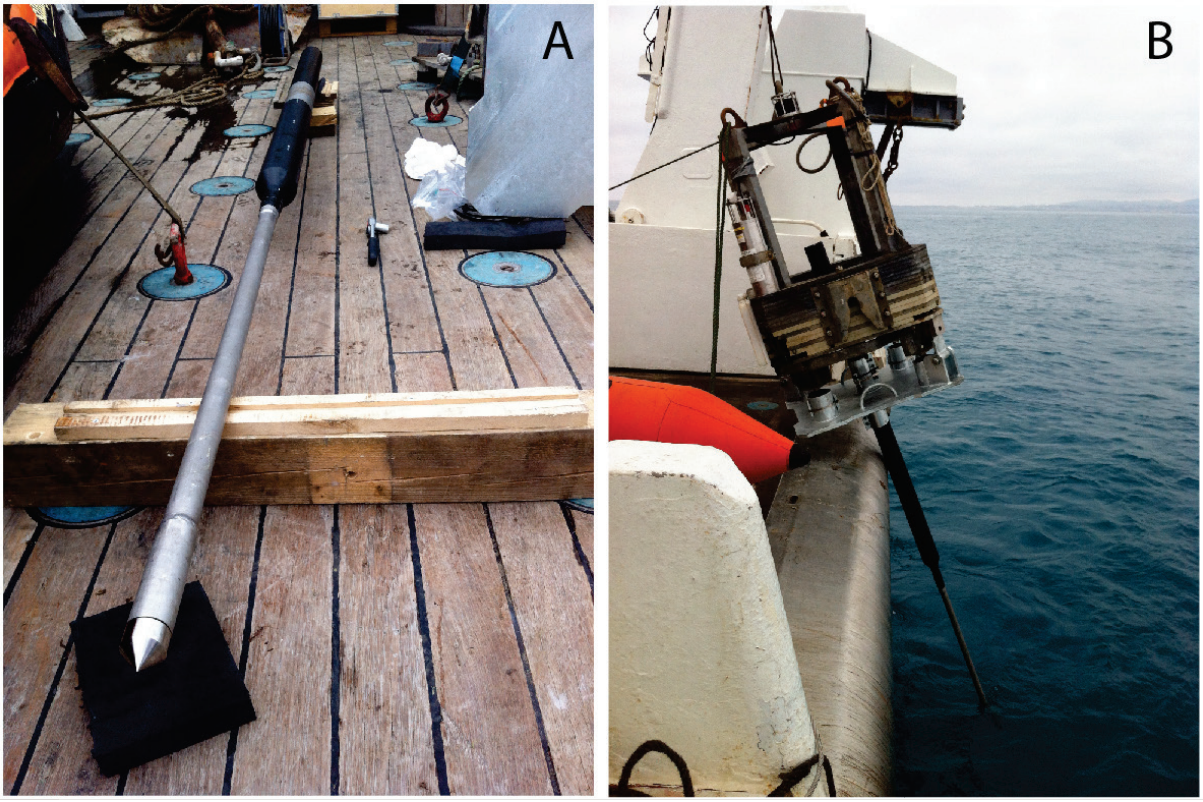

Fig. 19: MeBoPUPPI observatory with lance-shaped adapter and conical rod when assembled on deck of *RV L'Europe* (A) and when clamped to a base plate that is deployed by the weight stack (B). See text.

The aim of cruise POS500 is to recover this instrument, and also use a second, refined version for shorter term deployments during POS500.

5.6.2 Long-term Piezometer prototype

The pore pressure lance, or piezometer, is a refined version of an earlier prototype which was deployed suring cruise MSM35T and recovered during Pos498 (see Sahling et al., 2016). It has a heavy steel wheel as weight to obtain momentum for penetration, on top of which a steel cylinder that hosts the actual sensor package, is mounted. At its base, an appx. 3 m long steel lance with inside pressure tubing has been mounted. At the top, the steel cylinder holds a pressure housing with transducers measuring different parameters, such as:

1. tilting of the instrument (using triaxial ±1,7g MEMS accelerometers by Analog Devices)
2. internal temperature (Microchip type MCP9700) of the instrument housing
3. absolute pressure at the seafloor (KELLER RA-33X transducer, 25 MPa)
4. differential pressure between the seafloor and 3 m below the seafloor (tip of the p-lance in the sediment) using a KELLER PD-33X transducer (±500 kPa).

All data are logged in a self-contained mode using a commercial RBR Concerto data logger, which is usually set at a rate of 1 min^{-1}.

The device was located on the seafloor and successfully recovered during a dive with the MARUM ROV Squid during expedition P498 (Fig. 20). It remained on the vessel and was refurbished during POS500 for its next deployment in the Western Mediterranean Sea.

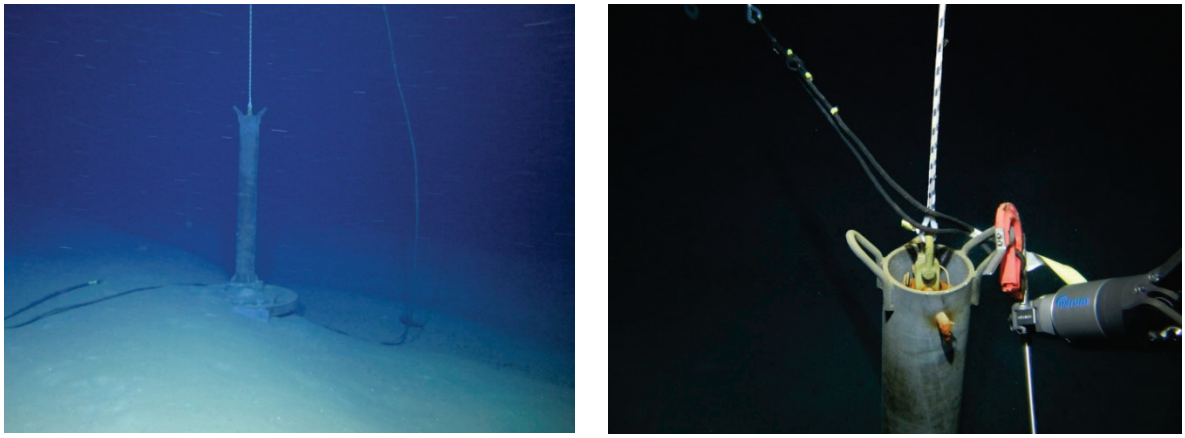

Fig. 20: Pore pressure lance as found and hooked to the ship's cable during cruise P498 (upper photos) and during recovery on deck (s. next page). Also see Sahling et al. (2016) for details.

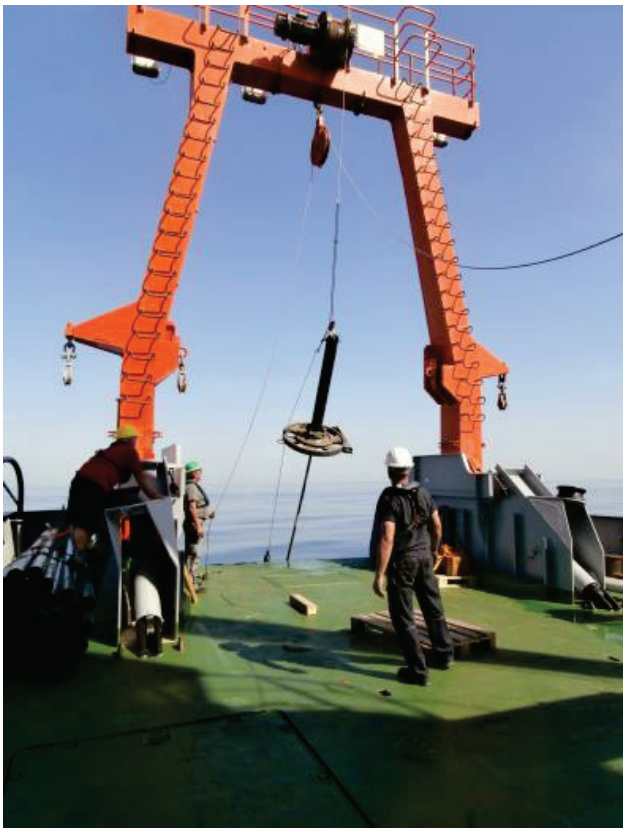

Fig. 20 continued. See previous page for caption.

5.6.3 Long-term Temperature probe

Similar to the piezometer probe, the T probe is an in-house development by the University of Bremen by utilising commercial off-the-shelf products as well as custom-made parts. The top of the probe contains a weight set made of a metal barrel filled with concrete and steel to provide the probe wit sufficient momentum for the free-fall deployments. A 5m-long steel rod with a violin-bow type thermistor string is screwed to the top weight. Eight thermistors, equally spaced on a string spanning the full 5 m length of the probe, enable the user to obtain T gradients over time. Data are logged by a commercial RBR data logger at a rate of 1 min^{-1}.

The device was located on the seafloor and successfully recovered during a dive with the MARUM ROV Squid during expedition P498 (Fig. 21). It remained on the vessel and was refurbished during POS500 for its next deployment in the Western Mediterranean Sea.

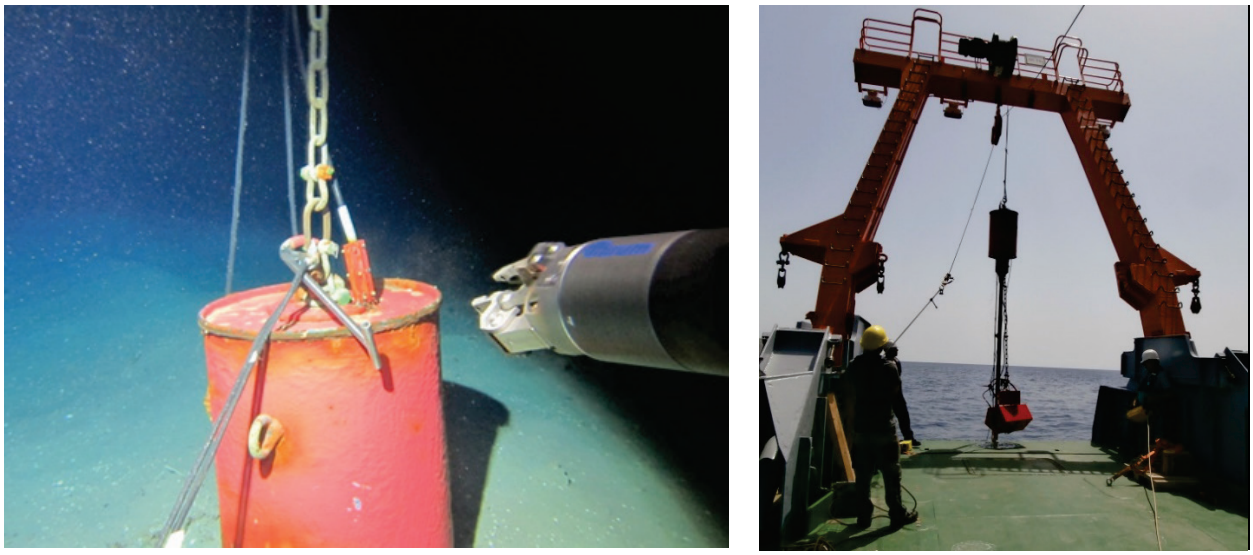

Fig. 21: Long-term T lance as found on the seafloor during cruise P498 (left) and upon retrieval on aft deck of RV Poseidon (Sahling et al., 2016).

6. Preliminary Results

The preliminary results from cruise POS500 can be divided into geophysical and geological ones: (i) AUV mapping and MCS survey, and (ii) coring, pore water extraction and bottom water sampling. In addition, recovery and relaunch of a long-term observatory were performed. We follow the structure of sub-chapters from the Methods section (Ch. 5) when presenting tentative cruise results.

6.1 ELAC MB and AUV bathymetric survey with MARUM SEAL 5000

6.1.1 ELAC Multibeam system

Over the course of cruise POS500, a fairly complete set of multibeam data was acquired (Fig. 23). The idea is to blend these data into existing bathymetric charts by MARUM and IFREMER, and also include the higher resolution AUV bathymetry (see below) post-cruise.

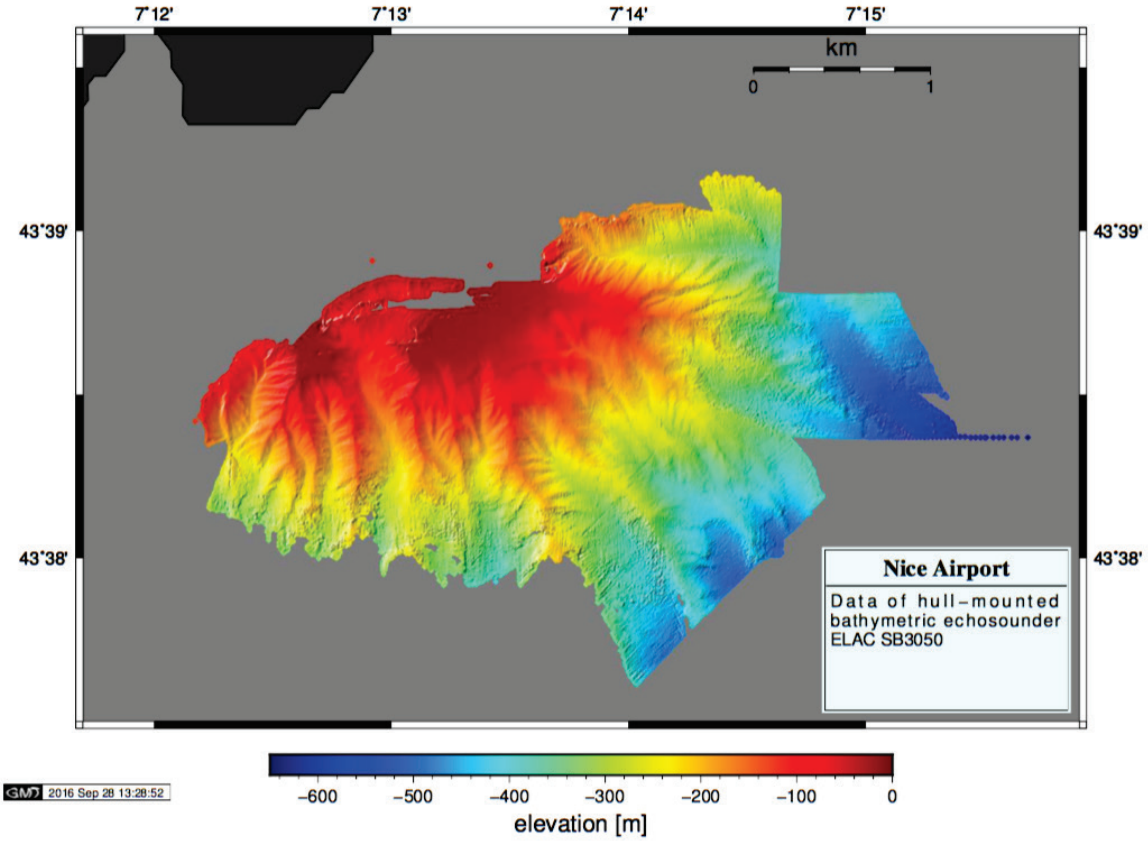

Fig. 23: ELAC Multibeam bathymetric map as acquired during cruise POS500.

6.1.2 AUV bathymetric survey with MARUM SEAL 5000

Station work on RV Poseidon cruise POS500

The scientific target area is lying southeasterly off the Nice airport, directly near shore. The expected water depth ranges from 135 m down to less than 10 m water depth. Actually, the target area has two major operational restrictions, i.e. the water depth limitation and the high abundance of surface crafts (slow speed fishing and high speed pleasure boats), crossing the AUV mission area from NNE to SSW and vice versa. Despite knowing the operational challenge to program an AUV mission into the shallow water depth, we have had the slight hope to do so. Unfortunately, the complete target area was equipped with several underwater fishnets of unclear orientation (buoy-indicator on surface). The presence of fishnets completely avoids the operation of the AUV in missions-mode (e.g. diving), due to high risk to become entangled in the nets. Finally, the only chance to operate the AUV was the operation in surface-mode. Even the surface mode and automated mission-mode of the AUV was not possible, due to almost "ad-hoc" presence and diagonal crossing of high-speed pleasure and commuter boats from offshore Mega-Yachts into Nice port. All these operational constraints end up in steering the AUV manually over the day and permanently parallel the AUV track with the zodiac (to minimise the chance to interfere with surface crafts). We did two missions over two days; on the third day the weather became to harsh to operate the AUV from RV Poseidon.

Dive/Mission No. 80:

The AUV was operated in the SSW lying part of the scientific area (splitted by fishnet buoys). The mission length has been nearly 7 hours and roughly 32 km of track line (Fig. 24). The strong relief in morphology has been a challenge, because no operational experience exists to operate the EM2040 in different frequencies and sounding ranges from 135 m to 5 m range (within a dive), which usually not occurs (it is an automated AUV-MBES and not an online MBES).

Dive/Mission No. 81:

The AUV was operated in the NNE lying part of the scientific area. The mission length has been 8 hours and roughly 40 km of track line (Fig. 25). Again, the strong relief in morphology has been a challenge in this area, as well.

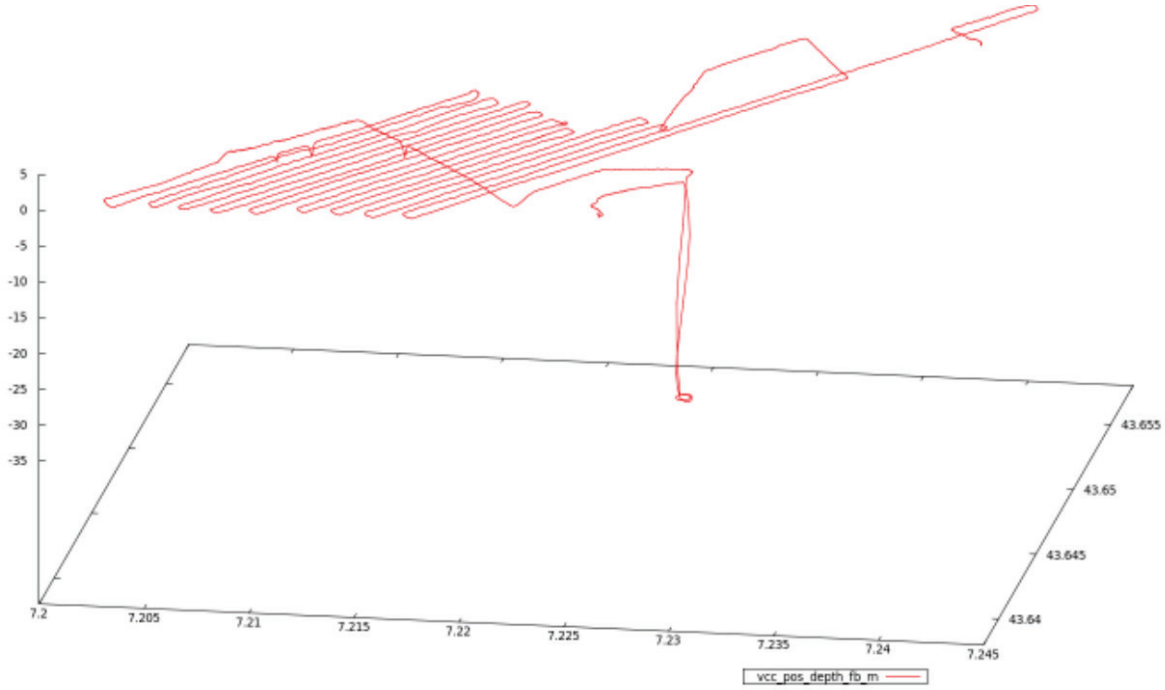

Fig. 24: Track line of surface-mission No. 80 of AUV MARUM SEAL, SW off Nice Airport.

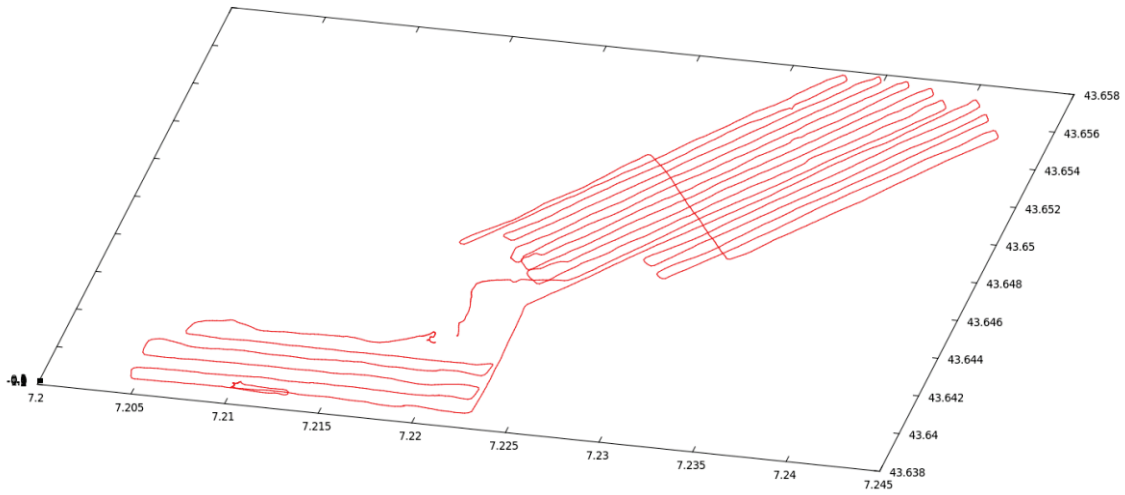

Fig. 25: Track line of surface-mission of AUV MARUM SEAL, SE and S off Nice Airport.

The combined track chart is seen in Figure 26.

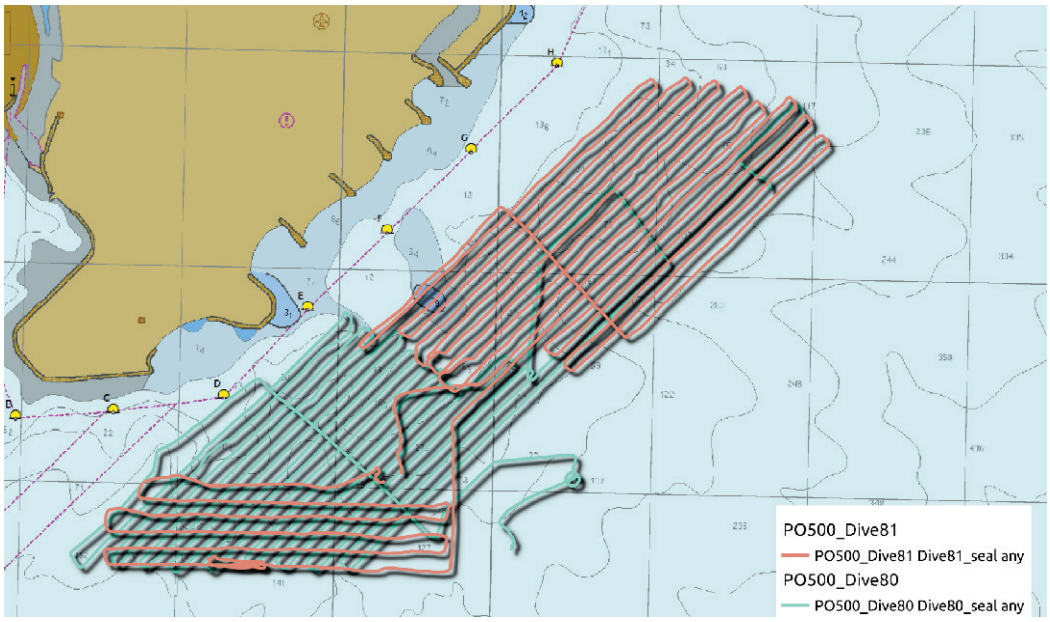

Fig. 26: Combined Track-lines of two-day AUV surface missions.

Figure 27 shows the AUV raw data from the combined mapping survey (Fig. 26). Processing will be done post-cruise.

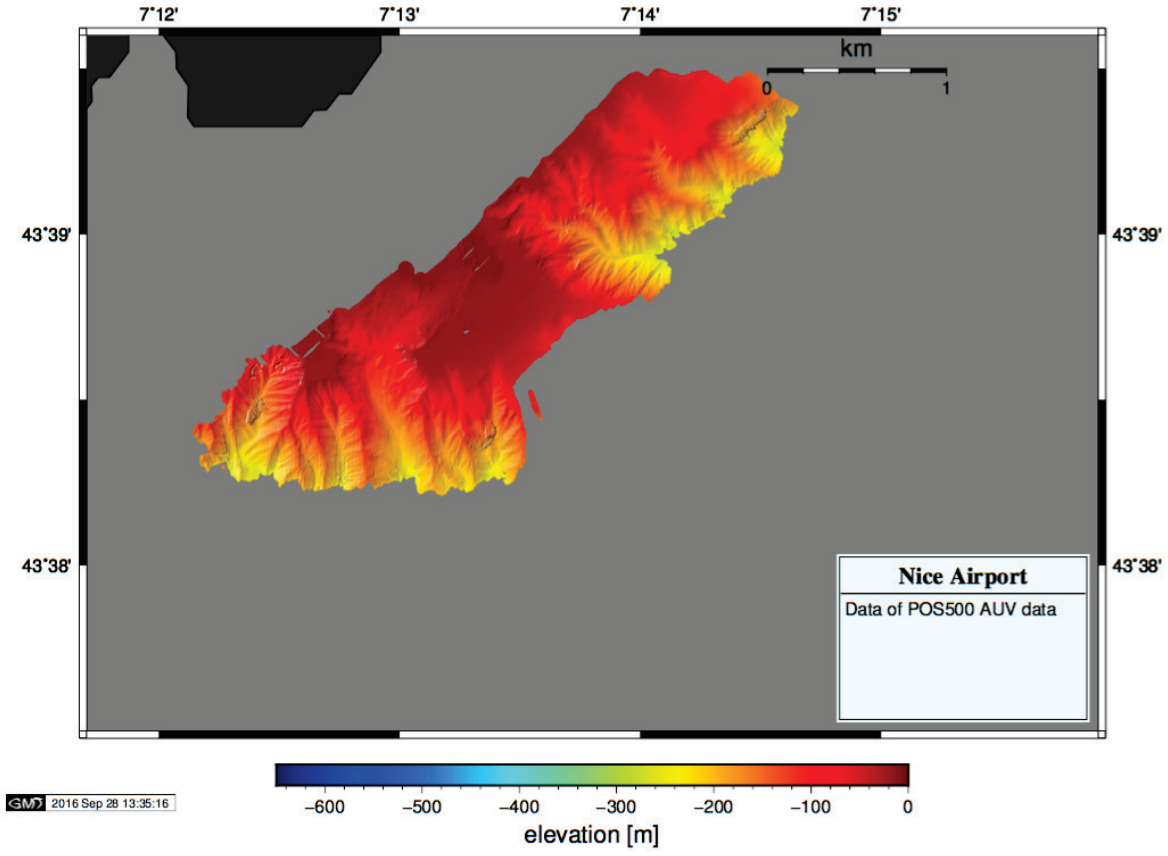

Fig. 27: GMT plot of the AUV map produced during POS500 cruise.

6.2 Gravity & push coring and sediment description

During cruise POS500, the science party comprised of mostly geophysicists and seagoing technology specialist so that cores were not split or described.

In this chapter we hence only note that a total of 9 gravity cores were taken. The recovery from each 6m-long gravity core is given in Table 1. In addition, 33 push cores using the MIC were recovered in order provide bottom water above the mud line and pore water below the mud line for geochemical analysis. These cores were not preserved and curated.

Table 1: Gravity cores taken during cruise POS500. For position, see station list (Ch. 8).

Core name	Recovery (cm)
GeoB21520-1	500
GeoB21521-1	400
GeoB21522-1	400
GeoB21553-1	577
GeoB21554-1	376
GeoB21555-1	476
GeoB21565-1	153
GeoB21566-1	331
GeoB21567-1	400

6.3 CTD and bottom water sampling

During cruise POS500, the CTD measurements, bottom water sampling and the analyses of bottom waters and interstitial fluids from the Mini-Push corer (MIC) were closely associated. We hence give a general introduction of how the sampling was done in this section, but report on geochemical fluid analysis in the next section (Ch. 6.4).

Figure 28 shows all the loci of CTD and Niskin water sampler deployment (see orange and red symbols), and additionally the gravity cores (see previous section) from which pore waters got extracted (see Ch. 6.4). Green symbols as well as some associated CTD data show mini-coring sites from which bottom and pore water got extracted. In order to study the Var aquifer activity and potential submarine GW seepage, the only crucial parameter in the CTD data set is elctrical conductivity, which is a direct measure of salinity. We hence report such data together with the geochemical results in the upcoming section.

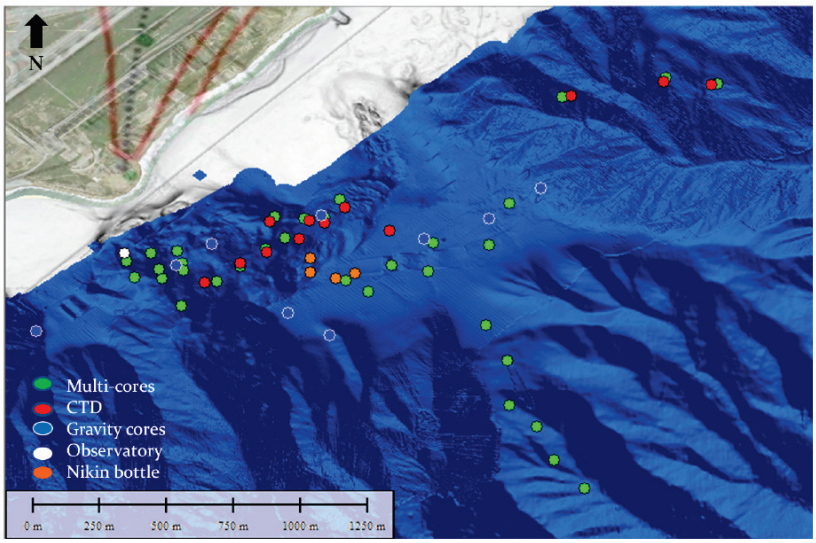

Fig. 28: Location of the sampling areas using different methods to sample water and/or sediment during the cruise POS500 offshore Nice.

6.4 Pore water geochemistry

Fluid analyses showed that freshening of the seawater is found both in the water column and in the interstitial fluids from MICs and GCs.

From AUV onboard CTD data, vertical profiles with the Niskin sampler-CTD unit as well as CTD runs mounted to the MIC we can identify a 3D distribution of freshening signals. Salinities lower than SW near the sealevel are interpreted as influence from the Var inflow into the Mediterranean. Freshened salinity near the sea bottom are interpreted as a product of submarine GW seepage. In these places, such GW charging is likely related to coarse-grained layers that gently dip oceanwards and pinch out at or very close to the sediment-water interface.

Compared to earlier cruises in the area, May 2016 turned out to be a period of enhanced seepage, which is attributed to the heavy rainfall in sping and also to the snow melt from the Maritime Alps. The seepage is a result of GW movement within the free aquifer, which is situated in the alluvial gravel onshore and accounts für appx. 80% of the Var aquifer movement (Potot, 2011). These groundwaters are then funneled into granular layers of cm- and dm-thickness in the marine sediments. In the gravity and opush cores, we sometimes reach such layers, most prominently in the 1979 landslide scar (e.g. GeoB21553 and -554) and the seaward edge of the metastable shelf plateau (e.g. GeoB21555). As illustrated in Figure 29, the freshening is fairly prominent in the scar (down to 5 per mil salinity) and less pronounced on the plateau edge (appx. 30 per mil).

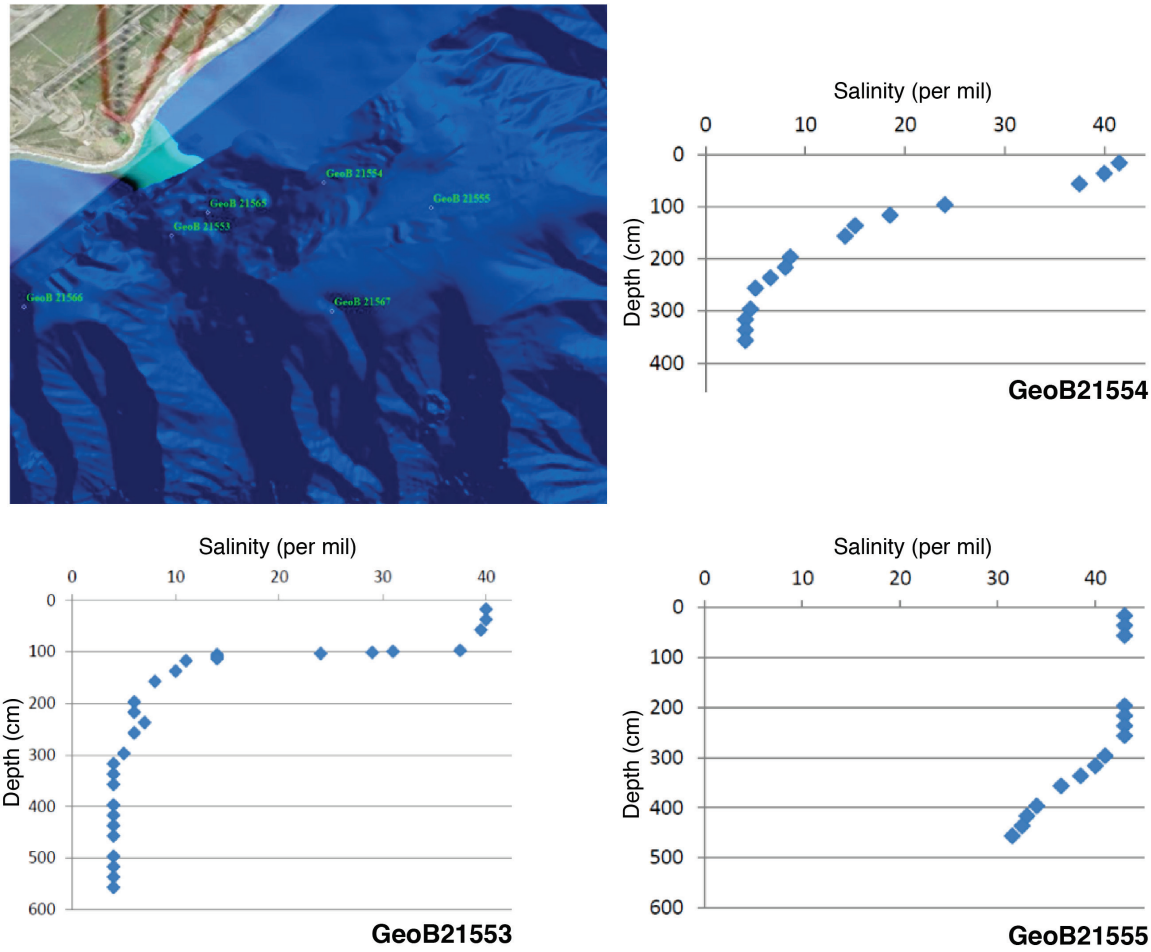

Fig. 29: Selected results from pore water salinity from cores of the western (GeoB21553) and eastern (GeoB21554) landslide scar as well as the southeastern edge of the plateau (GeoB21555) surrounding the scar. For locations of the sites, see map. Unpubl. data by Tugdual Gauchery.

In a study combining the onboard refractometer analyses with post-cruise ICP-OES (Inductively Coupled Plasma-Optical Emission Spectrometry) work, concentrations of various major and minor constitents got analysed in both the bottom waters and pore fluids (Gauchery, 2016). It can be seen from a simple contour plot that dilution from GW seepage affects up to >10 elements of the suite analysed, and is concentrated in the 1979 NAIL scar as well as the outermost shelf edge (Fig. 30).

There is also a spot somewhat further downslope at 43.641°N and 7.225°E where freshening is found in a depression which may represent a small landslide scar in >100m water depth. If this dilution is attributed to flow in the upper (i.e. free aquifer), it requires a profound hydraulic gradient to enable seepage in such a large water depth.

For details concerning the geochemical analyses on all waters from cruise POS500, refer to the Master thesis of Tugdual Gauchery (2016).

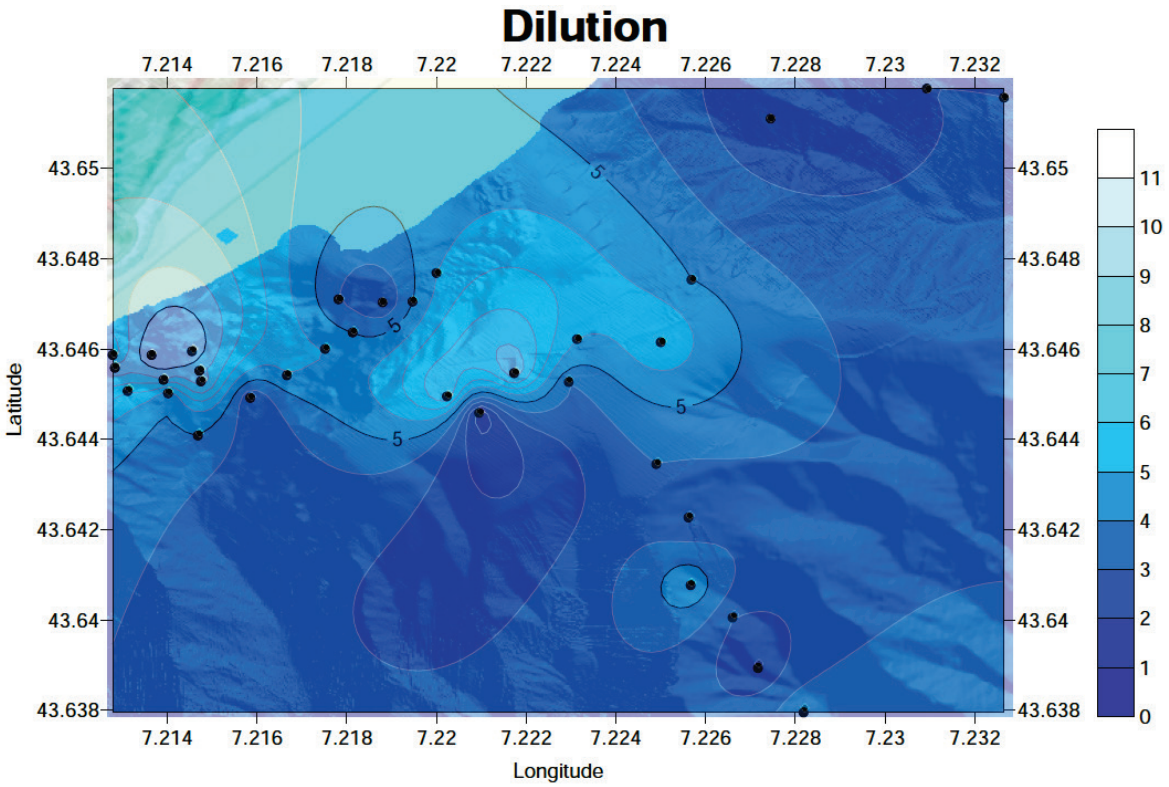

Fig. 30: Spatial distribution of dilution owing to GW movement an seepage in the study area. The shading (right bar) represents the number of elements which are depleted relative to SW. Modified after Gauchery (2016).

6.5 MCS reflection survey

In total 68 multichannel seismic lines were shot during cruise POS500. The overall data quality is very good, also due to the very quiet weather conditions during the survey. The survey grid during POS500 was designed for the high resolution imaging of the mass wasting scar in the study area. In order to acquire sufficient multichannel seismic data for subsequent 3D data processing and interpretation, a dense grid of E-W oriented profiles was acquired with a line spacing of 25 m. The acquired grid contains 55 profiles of which 10 lines were shot to repeat profiles of insufficient data quality. The remaining profiles were acquired as N-S lines over the area of interest as well as some slope-perpendicular profiles in the northern part of the study area (Fig. 31).

Onboard processing of seismic data was carried out using the commercial software package VISTA for Windows (Schlumberger). All profiles were preliminarily processed as brute stacks. After the preliminary processing the brute stacked data was loaded into our commercial seismic interpretation system The Kingdom Software (IHS).

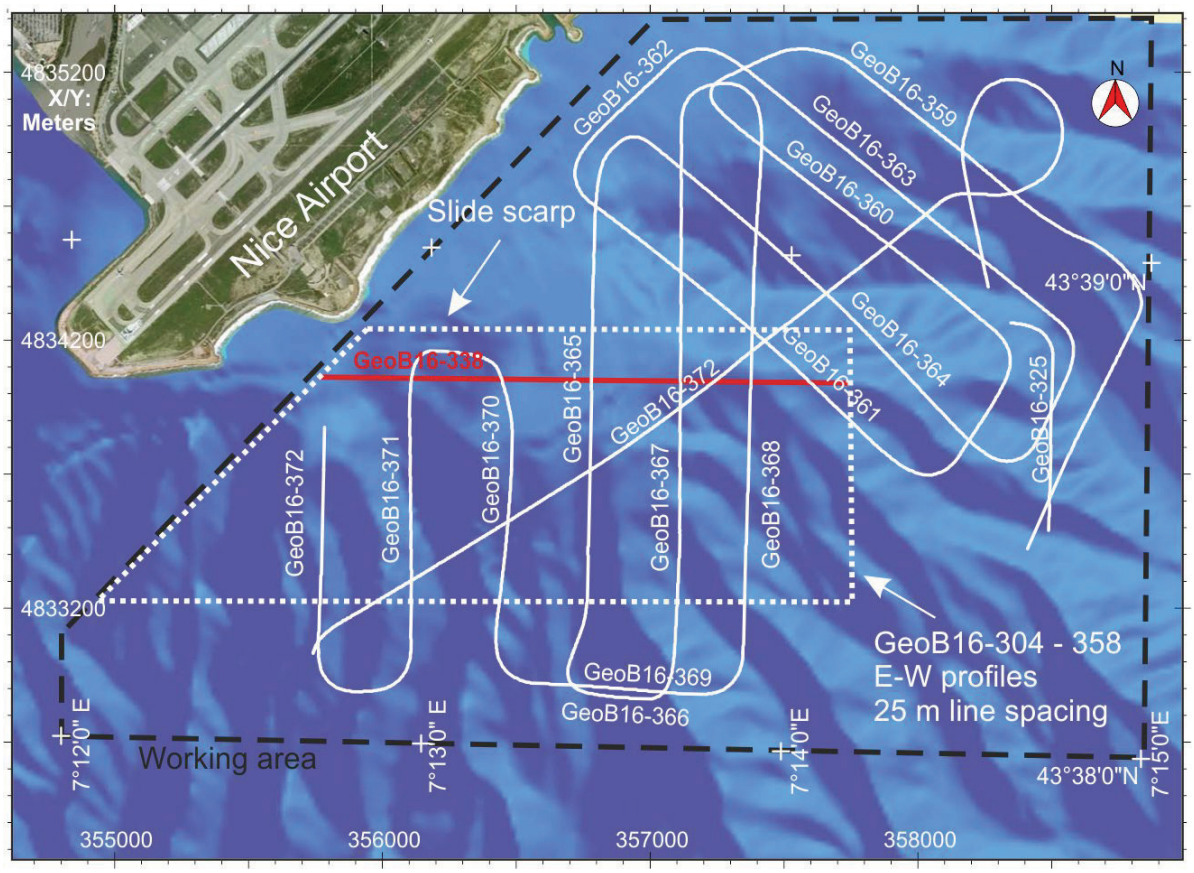

Fig. 31: Map of acquired multichannel seismic profiles. Stipled area shows the extent of densely spaced (25 m) seismic profiles to be included in a 3D data volume covering the mass wasting scar as well as the surrounding areas of stable shelf.

The aim of the multichannel seismic measurements was an improved imaging of the slump scar as well as the structure of neighboring areas of the shelf. For an optimal imaging of small-scale geological structures, 55 profiles were acquired in E-W orientation over the area of origin of the mass wasting event (Fig. 31). This dense grid of multichannel seismic lines will be used for 3D seismic data interpretation which will yield high resolution insights into the sub-seafloor geology and mechanisms for seafloor failure at this location. Additionally, 13 profiles were acquired in varying orientations perpendicular to the shoreline to provide additional data coverage over the working area.

The acquired seismic data is of excellent quality and shows signal penetration of ~400 ms in this geologically complex area. The source frequency bandwidth is between 100 and 400 Hz with a central frequency of 200 Hz. Thus, the expected vertical resolution of the data is between 2-4 m. A typical data example of the multichannel seismic measurements can be seen in the brute stack of profile GeoB16338 (Fig. 32). The shelf sediments show parallel seaward dipping reflectors, indicating prograding and aggrading shelf sequences. The scar of the mass wasting event can be seen in the western part of the profile (Fig. 32). A set of high amplitude reflectors could be imaged about 30 – 120 ms below the seafloor. These reflectors

also dip seawards and probably correspond to an older Pleistocene or Pliocene shelf surface. Amplitude variations in these reflectors may be due to the varying thickness of overlying sediments which also may be of varying lithology and potentially highly attenuating (e.g. gravel layers).

Further interpretation of the acquired data will be possible after the 3D processing of the data. Once this processing is achieved, the data will allow much more detailed geologic interpretation of the mass wasting complex than previously available data.

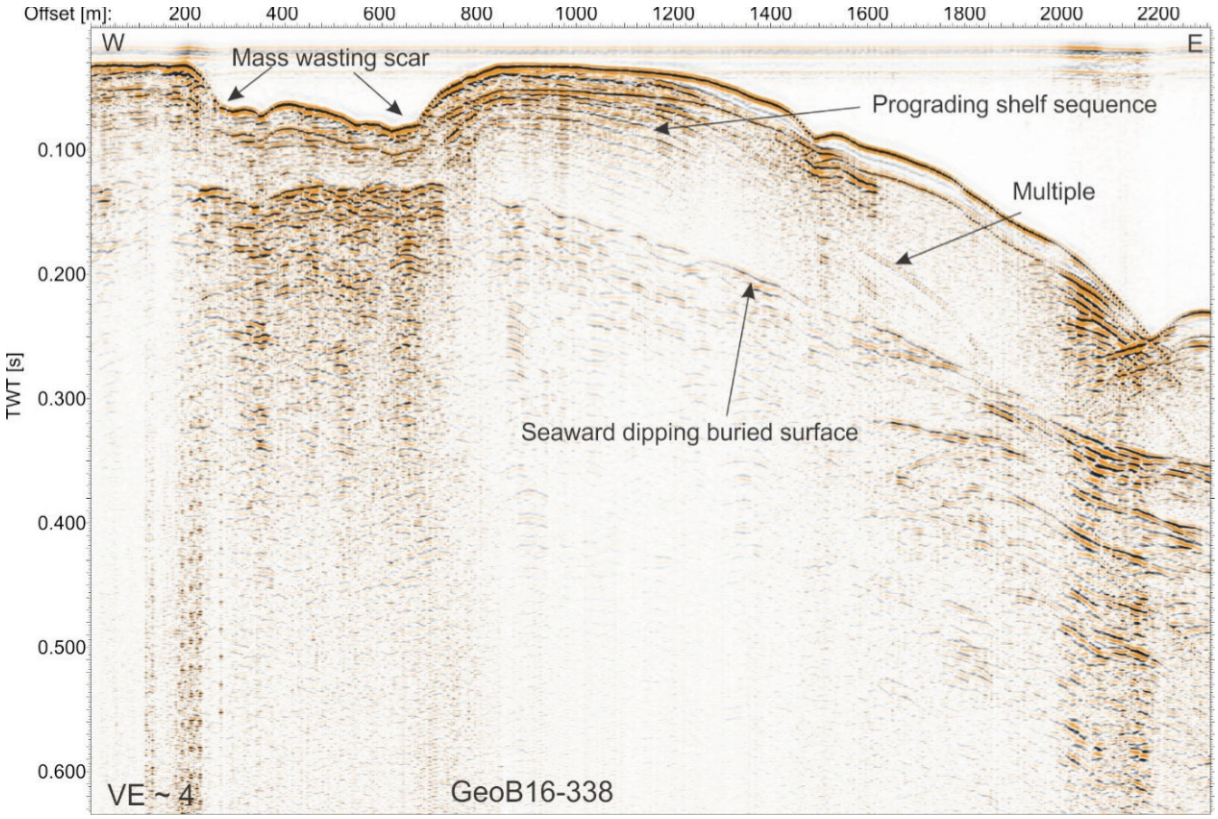

Fig. 32: Brutestack of multichannel seismic profile GeoB16-338. See **Fig. 31** for location. The signal penetration of the data is about 400 ms TWT. A set of seaward dipping reflectors is overlain by a prograding shelf sequence. The headwall area of the mass wasting event can be seen in the western part of the profile.

6.6 Long-term observatory tests

As explained in the Methods section (Ch. 5.6. above) we had different types of prototype observatories available during cruise POS500. The first important task was to recover the MeBoPUPPI piezometer probe that was deployed in May 2015 during IFREMER cruise STEP V, and where an evaluation of the performance of specific components of the observatory were a foremost goal. Given that the probe was deployed

using the IFREMER weight stack with a custom-made base plate into which the instrument was mounted (Fig. 19) we needed scuba divers to locate the device at the seafloor and shackle a ship's wire to it. When successfully on deck (Fig. 33), the instrument was cleaned and data were downloaded.

Fig. 33: MeBoPUPPI piezometer on its way back to the main deck of RV Poseidon (left) and then on deck after some maintenance to its outer hull, which showed corrosion (right).

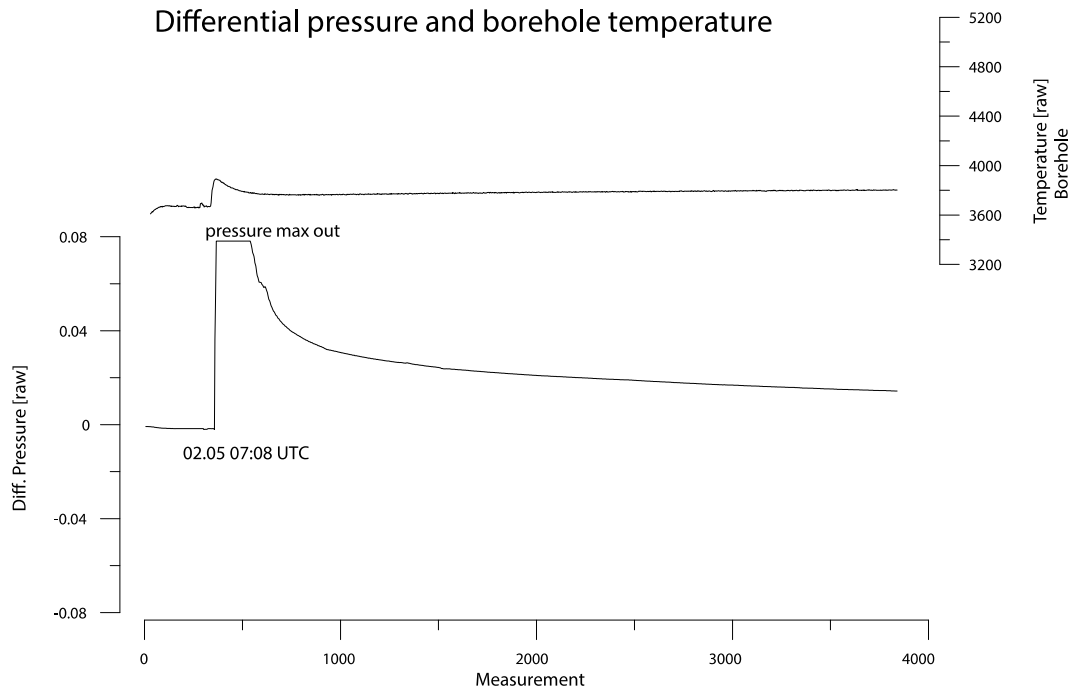

Fig. 34: Overview plot of MeBoPUPPI data immediately after its deployment in May 2015. Note that, owing to a technical error whose cause is yet to be analysed, only 10 days worth of data were recorded/retrieved.

As can be seen from Figure 34, the STEP V MeBoPUPPI prototype was deployed in the morning of 02 May 2015. As a function of the rigorous impact of the probe when still attached to the weight set, the differential pressure sensor maxed out while the temperature gave a nice reading of frictional heating. Both signals show a slow, gradual decay with time (Fig. 34), but no other significant trend or event-based excursions during the 10 days of operation. The instrument failed to record data after 11 May 2015 for reasons to be assessed post-cruise.

Towards the end of cruise POS500, we had a chance to deploy a refined version of the MeBoPUPPI instrument (station GeoB21571). At first glance, everything has worked.

7. References

Bennett, R.H., Li, H., Valent, P.J., Lipikin, J. and Esrig, M.I., 1985. In-Situ Undrained Shear Strengths and Permeabilities Derived from Piezometer Measurements, Strength Testing of Marine Seidments: Laboratory and In-Situ Measurements, ASTM STP 883, R.C. Chany and K.R. Demars, Ed., American Society for Testing and Materials, Philadelphia, pp.83-100.

Béthoux N., Ouillon G., Nicolas M., 1998. The instrumental seismicity of the Western Alps: spatiotemporal patterns analysed with the wavelet transform. Geophys. J. Int., 135, 1, 177-194.

Bjerrum, L., 1967. Progressive failure in slopes of overconsolidated plastic clay and clay shales. Journal of the Soil Mechanics and Foundation Division of the American Society of Civil Engineers, 93: 1-49.

Clauzon, G., 1981. C.R. Acad. Sci., Paris, 293, II, 309-314

Dan, G., Sultan, N., Savoye, B., 2007. The 1979 Nice Harbour Catastrophe revisited: Trigger mechanism inferred from geotechnical measurements and numerical modelling, Marine Geology, 245: 40-64.

Dubar, M., Anthony, E.J., 1995. Holocene Environmental Change and River-Mouth Sedimentation in the Baie des Anges, French Riviera. Quaternary Research, 43: 329-343

Emily A., Tennevin G., Mangan, C., 2010. Etude hydrogéologique des nappes profondes de la Basse Vallée du Var. Conseil Général Alpes Maritimes, 53pp.

Féraud, G. et al., 2009. Trace elements as geochemical markers for surface waters and groundwaters of the Var River catchment (Alpes Maritimes, France). Comptes Rendus Chimie, 12(8): 922-932.

Gauchery, T., 2016. Side effects of the 1979's landslide (Nice, France) on the submarine groundwater discharge and their consequences. Unpubl. MSc tesis, Univ. Bremen, 95pp.

Guglielmi, Y., 1993. Hydrogéologie des aquifères plio-quaternaires de la basse vallée du Var (Alpes-Maritimes, France). Thèse Université d'Avignon et des Pays de Vaucluse: 178p.

Guglielmi, Y., Prieur, L., 1997. Locating and Estimating submarine freshwater discharge from an interstitial confined coastal aquifer by measurements at sea: example from the lower Var Valley, France. Journal of Hydrology, 190: 111-122

Hampton, M.A., Lee, H.J., 1996. Submarine Landslides. Reviews of Geophysics, 34: 33-59.

Irr, F., 1984. Paléoenvironnements et évolution géodynamique néogène et quaternaire de la bordure nord du bassin méditerrannéen occidental, Nice, 464 pp.

Klaucke, I., Cochonat, P., 1999. Analysis of past seafloor failures on the continental slope off Nice (SE France). Geo-Mar Lett 19: 245-253.

Klaucke, I., Savoye, B., Cochonat, P., 2000. Patterns and processes of sediment dispersal on the continental slope off Nice, SE France. Mar Geol 162: 405-422.

Kopf, A., Stegmann, S., Krastel, S., Förster, A., Strasser, M, Irving, M., 2007. Marine deep-water Free-fall CPT measurements for landslide characterisation off Crete, Greece (Eastern Mediterranean Sea) --- PART 2: Initial data from the western Cretan Sea. In: Lykousis, V., Sakellariou, D., Locat, J. (eds.), Submarine Mass movements and their consequences. Advances in Natural and Technological Hazards Series, Springer, 199-208.

Kopf, A., and shipboard party, 2008. REPORT AND PRELIMINARY RESULTS OF METEOR CRUISE M73/1: LIMA-LAMO. Berichte aus dem Fachbereich Geo-wissenschaften der Univ. Bremen, No. 264: 169pp.

Kopf, A., Kasten , S., Blees, J., 2009. Geochemical evidence for groundwater-charging of slope sediments: The Nice Airport 1979 landslide and tsunami revisited. Proc. IGCP511, Submarine mass movements and their consequences, Houston (TX), 203-214.

Kopf, A., and shipboard party, 2009. REPORT AND PRELIMINARY RESULTS OF POSEIDON CRUISE P386: NAIL (Nice Airport Landslide), Berichte aus dem Fachbereich Geowissenschaften der Univ. Bremen, No. 271: 161pp

Kopf, A., Delisle, G., Faber, E., Panahi, B., Aliyev, C.S., Guliyev, I., 2010. Long-term in situ monitoring at Dashgil mud volcano, Azerbaijan: A link between seismicity, pore pressure transients and methane emission. Int. J. Earth Sciences, 99: 227-240.

Kopf, A., Araki, E., Toczko, S., and the Expedition 332 Scientists, 2011a. Proc. IODP, Initial Reports 332: Washington, DC (Integrated Ocean Drilling Program Management International, Inc.), 190 pp. doi: 10.2204/iodp.proc.332.2011

Kopf, A., Freudenthal, T., Ratmeyer, V., Bergenthal, M., Lange, M., Fleischmann, T., Hammerschmidt, S., Seiter, C., and Wefer, G., 2015. Simple, affordable, and sustainable borehole observatories for complex monitoring objectives, Geosci. Instrum. Method. Data Syst., 4, 99-109, doi:10.5194/gi-4-99-2015

Kopf A., Sylvia Stegmann, Sebastien Garziglia, Nabil Sultan, Pierre Henry, Bernard Dennielou, Simon Haas, Kai-Christian Weber, 2016. Soft sediment deformation in the shallow submarine slope off Nice (France) as a result of a variably charged Pliocene aquifer and mass wasting processes. Sedimentary Geology, DOI: j.sedgeo.2016.05.014

Larroque, C., Bethoux, N., Calais, E., Courboulex, F., Dechamps, A., Deverchere, J., Stephan, J.F., Ritz, J.F., Gilli, E., 2001. Active and recent deformation at the Southern Alps – Ligurian basin junction. Netherlands J. Geosci., Geol., Mijnbouw, 80: 255-272.

Laurent O., Stephan, J.F. and Popoff, M., 2000. Modalités de la structuration miocène de la branche sud de l'arc de Castellane (chaines subalpines méridionales), Géologie de la France, 3, 33–65.

Lee, H.J., 2009. Timing of occurrence of large submarine landslides on the Atlantic Ocean margin. Marine Geology 264: 53-64

Leroueil, S., 2001. Natural slopes and cuts: movement and failure mechanisms. Geotechnique, 51: 197-243

Locat, J. & Lee, H. J., 2002. Submarine landslides: Advances and challenges. Canadian Geotechnical Journal, 39:193

Maltman, A. (Ed.), 1994. The Geological Deformation of Sediments. Chapman & Hall, London, 363pp.

Maslin, M., Owen, M., Day, S., Long, D., 2004. Linking continental-slope failures and climate change: testing the clathrate gun hypothesis. Geology 32: 53–56

Migeon, S., Cattaneo, A., Hassoun, V., Dano, A., Casedevant, A., Ruellan, E., 2012. Failure Processes and Gravity-Flow Transformation Revealed by High-Resolution AUV Swath Bathymetry on the Nice Continental Slope (Ligurian Sea). In: Submarine Mass Movements and Their Consequences: Advances in Natural and Technological Hazards Research, Volume 31: 451-461

MIP, 1981. Mission d'Inspection Pluridisciplinaire sur le sinistre de Nice du 16 Octobre 1979 - Rapport final. Unpublished report.

Moore, C.J. & science party, 1995. Abnormal fluid pressures and fault-zone dilation in the Barbados accretionary prism: Evidence from logging while drilling. Geology, 23/7, 605-608.

Mulder, T., Savoye, B., Syvitski, J.P.M., 1997. Numerical modelling of a mid-sized gravity flow: the 1979 Nice turbidity current (dynamics, processes, sediment budget and seafloor impact). Sedimentology, 44: 305-326.

Mulder, T., Savoye, B., Syvitski, J.P.M., and Piper, D.J.W. 1998. The Var Submarine System: understanding Holocene sediment delivery processes and their importance to the geological record. In: Stoker, M.S., Evans, D. and Cramp, A. (Eds.), Geological Processes on Continental Margins: Sedimentation, Mass Wasting and Stability. Spec. Publ. Geol. Soc. London, pp. 145-166

Oehler, T., 2011. A Geochemical Study on Fluid Dynamics within a Landslide Scar off Nice. Unpubl. MSc thesis, Univ. Bremen, Germany, 128 pp.

Pautot, G., 1981. Cadre morphologique de la Baie des Anges. Mode`le d'instabilite´ de pente continentale. Oceanol. Acta 4: 203–212

Petley, N.D., Higuchi, T., Petlet, D., Bulmer, H.M., Carey, J., 2005. Development of progressive landslide failure in cohesive materials. Geology, 33: 201-204

Potot, C., 2011. Etude hydrochimique du systeme aquifere de la basse vallee du Var. PhD thesis, Univ. Nice Sophia-Antipolis, 240pp

Rehault J. P., Boillot G., Mauffret A., 1984. The western Mediterranean basin: Geological evolution. Marine Geology, 55, 447-477.

Salichon, J., Kohrs-Sansorny, C., Bertrand, E., Courboulex, F., 2010. A Mw 6.3 earthquake scenario in the city of Nice (southeast France): ground motion simulations. Journal of Seismology 14, 3, 523-541, DOI : 10.1007/s10950-009-9180-0

Savoye, B., Piper, D., and Droz, L., 1993. Plio-Pleistocene evolution of the Var deep-sea fan off the French Riviera. Marine and Petroleum Geology, 10, 550-570.

Savoye, B., Piper, D.J.W., 1991. The Messinian event on the margin of the Mediterranean Sea in the Nice area, southern France. Marine Geology, 97: 279-304.

Seed, H. B., Seed, R. B., Schlosser, F., Blondeau, F., Juran, I. 1988. The Landslide at the port of Nice on October 16, 1979. Earthquake Engineering Research Center, report No. UCB/EERC-88/10

Stegmann, S., Moerz, T., Kopf, A., 2006. Initial Results of a new Free Fall-Cone Penetrometer (FF-CPT) for geotechnical in situ characterisation of soft marine sediments. Norwegian Journal of Geology, 86/3: 199-208.

Stegmann, S., Strasser, M., Anselmetti, F.S., Kopf, A., 2007. Geotechnical in situ characterisation of subaquatic slopes: The role of pore pressure transients versus frictional strength in landslide initiation. Geophysical Research Letts., 34/7, doi:10.1029/2006GL029122.

Stegmann, S., Sultan, N., Kopf, A., Apprioual, R., Pelleau, P., 2011. Hydrogeology and its effect on slope stability along the coastal aquifer of Nice, France. Marine Geology, 280: 161-181.

Stegmann, S., Sultan, N., Pelleau, P., Apprioual, R., Garziglia, S., Kopf, A., Zabel, M., 2012. A long-term monitoring array for landslide precursors. A case study at the Ligurian Slope. OTC Proceedings, Houston April 2012, paper number OTC-23271-PP

Stegmann, S., Kopf, A., 2013. How stable is the Nice slope? – An analysis based on strength and cohesion from ring shear experiments. In Krastel, S., et al. (eds.), Proceedings 6th meeting of Submarine Mass Movements and their consequences, Springer: 189-200.

Sultan, N., Cochonat, P., Canals, M., Cattaneo, A., Dennielou, B., Haflidason, H., Laberg, J.S., Long, D., Mienert, J., Trincardi, F., Urgeles, R.,Vorrene, T.O.,Wilson, C., 2004. Triggering mechanisms of slope instability processes and sediment failures on continental margins: a geotechnical approach. Marine Geology, 213, 291–321

Sultan, N., and shipboard party, 2008. Prisme Cruise (R/V Atalante Toulon - Toulon; 2007): Reports and Preliminary Results. IFREMER Internal Report, Ref: IFR CB/GM/LES/08-11, 180pp.

Sultan, N., Savoye, B., Jouet, G., Leynaud, D., Cochonat, P., Henry, P., Stegmann, S., Kopf, A., 2010. Investigation of a possible submarine landslide at the Var delta front (Nice-slope—SE France). Canadian Geotechnical Journal 47: 486–496.

Terzaghi, K., 1925. Erdbaumechanik auf bodenphysikalischer Grundlage, Franz Deuticke, Leipzig, Germany, pp. 399

Waldmann, C., Freudenthal, T., Kopf, A., 2014. Underwater monitoring network: Using the deep-sea Drill MARUM-MeBo for installing Subseafloor Sensor Systems for monitoring Seafloor Intervention Operations. Proc. Offshore Technology Conference held in Houston, Texas, USA, 5–8 May 2014, paper OTC 25301

8. Station list

GeoB	Ship Site Number		Date	Time	Position Lat	Position Long	Water Depth [m]	Gear
21501-1	POS500_197-1	Start	28.05.16	08:03	43° 38,36' N	007° 13,57' E	0	AUV
		End	28.05.16	15:09	43° 39,20' N	007° 14,37' E	0	AUV
21503-1	POS500_198-1	Bottom	28.05.16	16:25	43° 38,75' N	007° 12,80' E	37	MIC
21503-2	POS500_198-2	Bottom	28.05.16	16:35	43° 38,74' N	007° 12,81' E	44,7	CTD
21504-1	POS500_199-1	Bottom	28.05.16	16:53	43° 38,70' N	007° 12,84' E	62,4	MIC
21504-2	POS500_199-2	Bottom	28.05.16	16:58	43° 38,69' N	007° 12,85' E	63,2	CTD
21505-1	POS500_200-1	Bottom	28.05.16	17:11	43° 38,65' N	007° 12,88' E	4,6	MIC
21505-2	POS500_200-2	Bottom	28.05.16	17:16	43° 38,65' N	007° 12,89' E	93,1	CTD
21506-1	POS500_201-1	Start	29.05.16	06:26	43° 38,55' N	007° 13,22' E	0	AUV
		End	29.05.16	14:44	43° 38,51' N	007° 13,16' E	0	AUV
21507-1	POS500_202-1	Bottom	29.05.16	16:13	43° 38,69' N	007° 13,20' E	14,4	MIC
21507-2	POS500_202-2	Bottom	29.05.16	16:16	43° 38,69' N	007° 13,20' E	13,7	CTD
21508-1	POS500_203-1	Bottom	29.05.16	16:29	43° 38,68' N	007° 13,26' E	15,2	MIC
21508-2	POS500_203-2	Bottom	29.05.16	16:33	43° 38,67' N	007° 13,25' E	15,5	CTD
21509-1	POS500_204-1	Bottom	29.05.16	16:43	43° 38,72' N	007° 13,30' E	13,2	MIC
21509-2	POS500_204-2	Bottom	29.05.16	16:46	43° 38,73' N	007° 13,31' E	12,6	CTD
21510-1	POS500_205-1	Bottom	29.05.16	16:59	43° 38,72' N	007° 13,38' E	17	MIC
21510-2	POS500_205-2	Bottom	29.05.16	17:03	43° 38,71' N	007° 13,38' E	17,5	CTD
21511-1	POS500_206-1	Bottom	29.05.16	17:11	43° 38,77' N	007° 13,39' E	15,2	MIC
21511-2	POS500_206-2	Bottom	29.05.16	17:13	43° 38,77' N	007° 13,39' E	15,1	CTD
21512-1	POS500_207-1	Bottom	29.05.16	17:20	43° 38,77' N	007° 13,50' E	19,6	MIC
21512-2	POS500_207-2	Bottom	29.05.16	17:24	43° 38,78' N	007° 13,51' E	20,6	CTD
21513-1	POS500_208-1	Bottom	29.05.16	17:32	43° 38,85' N	007° 13,54' E	18,6	MIC
21513-2	POS500_208-2	Bottom	29.05.16	17:35	43° 38,87' N	007° 13,55' E	20,1	CTD
21514-1	POS500_209-1	Bottom	29.05.16	18:06	43° 38,73' N	007° 12,83' E	45,6	MIC
21514-2	POS500_209-2	Bottom	29.05.16	18:09	43° 38,73' N	007° 12,83' E	49,9	CTD
21515-1	POS500_210-1	Bottom	29.05.16	18:17	43° 38,72' N	007° 12,84' E	54,6	MIC
21515-2	POS500_210-2	Bottom	29.05.16	18:20	43° 38,72' N	007° 12,84' E	54,9	CTD
21516-1	POS500_211-1	Bottom	29.05.16	18:38	43° 38,74' N	007° 12,77' E	41,9	MIC
21516-2	POS500_211-2	Bottom	29.05.16	18:41	43° 38,73' N	007° 12,78' E	44,6	CTD
21517-1	POS500_212-1	Bottom	29.05.16	18:56	43° 38,70' N	007° 12,79' E	54,6	MIC
21517-2	POS500_212-3	Bottom	29.05.16	19:11	43° 38,70' N	007° 12,80' E	57,6	CTD
21518-1	POS500_213-1	Bottom	29.05.16	19:27	43° 38,76' N	007° 12,87' E	28,1	MIC
21518-2	POS500_213-2	Bottom	29.05.16	19:31	43° 38,76' N	007° 12,87' E	29,9	CTD
21519-1	POS500_214-1	Bottom	29.05.16	19:40	43° 38,72' N	007° 12,89' E	45,9	MIC
21519-2	POS500_214-3	Bottom	29.05.16	19:49	43° 38,73' N	007° 12,89' E	43,4	CTD
21520-1	POS500_215-1	Bottom	30.05.16	06:38	43° 38,89' N	007° 13,60' E	27,5	GC
21521-1	POS500_215-2	Bottom	30.05.16	07:31	43° 38,82' N	007° 13,50' E	17,5	GC
21522-1	POS500_215-3	Bottom	30.05.16	08:29	43° 38,63' N	007° 13,09' E	14,5	GC
21523-1	POS500_215-4	Bottom	30.05.16	11:31	43° 38,61' N	007° 13,49' E	41,4	MIC
21523-2	POS500_216-1	Bottom	30.05.16	11:38	43° 38,60' N	007° 13,52' E	44,9	CTD
21524-1	POS500_217-1	Bottom	30.05.16	11:56	43° 38,54' N	007° 13,54' E	75,1	MIC + CTD
21525-1	POS500_218-1	Bottom	30.05.16	12:15	43° 38,45' N	007° 13,54' E	111,6	MIC + CTD
21526-1	POS500_219-1	Bottom	30.05.16	12:35	43° 38,40' N	007° 13,60' E	147,1	MIC + CTD
21527-1	POS500_220-1	Bottom	30.05.16	12:58	43° 38,34' N	007° 13,63' E	192,4	MIC + CTD
21528-1	POS500_221-1	Bottom	30.05.16	13:27	43° 38,28' N	007° 13,69' E	250	MIC + CTD
21529-1	POS500_222-1	Bottom	30.05.16	14:22	43° 39,10' N	007° 13,96' E	103,9	MIC + CTD

GeoB	Ship Site Number		Date	Time	Position Lat	Position Long	Water Depth [m]	Gear
21530-1	POS500_223-1	Bottom	30.05.16	14:39	43° 39,11' N	007° 13,86' E	82,1	MIC + CTD
21531-1	POS500_224-1	Bottom	30.05.16	14:52	43° 39,07' N	007° 13,65' E	81,4	MIC + CTD
21532-1	POS500_225-1	Bottom	30.05.16	16:07	43° 38,86' N	007° 13,20' E	16,1	MIC + CTD
21533-1	POS500_226-1	Bottom	30.05.16	16:17	43° 38,81' N	007° 13,16' E	26,1	MIC + CTD
21534-1	POS500_227-1	Bottom	30.05.16	16:32	43° 38,82' N	007° 13,15' E	26,4	MIC + CTD
21535-1	POS500_228-1	Bottom	30.05.16	16:39	43° 38,79' N	007° 13,11' E	33,6	MIC + CTD
21536-1	POS500_229-1	Bottom	30.05.16	16:50	43° 38,82' N	007° 13,07' E	27,9	MIC + CTD
21537-1	POS500_230-1	Bottom	30.05.16	17:01	43° 38,76' N	007° 13,05' E	48,2	MIC + CTD
21538-1	POS500_231-1	Bottom	30.05.16	17:08	43° 38,72' N	007° 13,00' E	58,1	MIC + CTD
21539-1	POS500_232-1	Bottom	30.05.16	17:16	43° 38,70' N	007° 12,95' E	62,6	MIC + CTD
21540-1	POS500_233-1	Start	31.05.16	07:30	43° 38,62' N	007° 12,92' E	100,6	MEBO OBS. 2015
		Bottom	31.05.16	08:06	43° 38,73' N	007° 12,83' E	47,9	MEBO OBS. 2015
		End	31.05.16	08:10	43° 38,75' N	007° 12,81' E	37,6	MEBO OBS. 2015
21541-1	POS500_234-1	Start	31.05.16	11:32	43° 38,82' N	007° 13,17' E	24,4	CTD
21542-1	POS500_235-1	Start	31.05.16	11:47	43° 38,84' N	007° 13,21' E	20,9	CTD
21543-1	POS500_236-1	Start	31.05.16	11:54	43° 38,82' N	007° 13,14' E	27,1	CTD
21544-1	POS500_237-1	Start	31.05.16	12:00	43° 38,79' N	007° 13,12' E	35,9	CTD
21545-1	POS500_238-1	Start	31.05.16	12:08	43° 38,81' N	007° 13,08' E	28,1	CTD
21546-1	POS500_239-1	Start	31.05.16	12:27	43° 38,75' N	007° 13,05' E	48,9	CTD
21547-1	POS500_239-2	Start	31.05.16	12:36	43° 38,72' N	007° 13,01' E	56,6	CTD
21548-1	POS500_240-1	Start	31.05.16	12:49	43° 38,69' N	007° 12,94' E	66,1	CTD
21549-1	POS500_241-1	Start	31.05.16	13:38	43° 39,09' N	007° 13,95' E	101	CTD
21550-1	POS500_242-1	Start	31.05.16	13:54	43° 39,10' N	007° 13,85' E	94,6	CTD
21551-1	POS500_243-1	Start	31.05.16	14:07	43° 39,07' N	007° 13,66' E	90,9	CTD
21552-1	POS500_244-1	Start	31.05.16	14:29	43° 38,80' N	007° 13,30' E	12	CTD
21553-1	POS500_245-1	Bottom	02.06.16	06:16	43° 38,73' N	007° 12,87' E	42,7	GC
21554-1	POS500_246-1	Bottom	02.06.16	06:58	43° 38,83' N	007° 13,16' E	23,6	GC
21555-1	POS500_247-1	Bottom	02.06.16	07:52	43° 38,77' N	007° 13,37' E	14,1	GC
21556-1	POS500_248-1	Start	02.06.16	08:33	43° 38,71' N	007° 13,23' E	14	NB+CTD
21557-1	POS500_249-1	Start	02.06.16	08:47	43° 38,70' N	007° 13,19' E	13,2	NB+CTD
21558-1	POS500_250-1	Start	02.06.16	08:58	43° 38,71' N	007° 13,15' E	10,5	NB+CTD
21559-1	POS500_251-1	Start	02.06.16	09:23	43° 38,74' N	007° 13,14' E	21,5	NB+CTD
21560-1	POS500_252-1	Start	02.06.16	11:40	43° 38,15' N	007° 12,17' E	292,2	SEISREFL
			02.06.16	11:54	43° 38,45' N	007° 12,51' E	103,3	SEISREFL
			02.06.16	12:00	43° 38,60' N	007° 12,71' E	39,7	SEISREFL
			02.06.16	12:35	43° 38,79' N	007° 13,92' E	183,3	SEISREFL
			02.06.16	13:06	43° 38,75' N	007° 12,98' E	45,4	SEISREFL
			02.06.16	13:34	43° 38,67' N	007° 13,90' E	119,4	SEISREFL
			02.06.16	14:05	43° 38,61' N	007° 13,15' E	100	SEISREFL
			02.06.16	14:20	43° 38,51' N	007° 13,85' E	189,5	SEISREFL
			02.06.16	14:34	43° 38,43' N	007° 12,32' E	146,6	SEISREFL
			02.06.16	14:49	43° 38,42' N	007° 13,91' E	243,1	SEISREFL
			02.06.16	15:11	43° 38,45' N	007° 12,43' E	162	SEISREFL
			02.06.16	15:29	43° 38,68' N	007° 14,18' E	206,8	SEISREFL
			02.06.16	15:54	43° 38,33' N	007° 12,54' E	157,4	SEISREFL
			02.06.16	16:11	43° 38,59' N	007° 14,16' E	189,6	SEISREFL
			02.06.16	16:30	43° 38,51' N	007° 12,69' E	74,8	SEISREFL
			02.06.16	16:46	43° 38,77' N	007° 14,03' E	110,7	SEISREFL

GeoB	Ship Site Number		Date	Time	Position Lat	Position Long	Water Depth [m]	Gear
			02.06.16	16:58	43° 38,65' N	007° 12,64' E	26,6	SEISREFL
			02.06.16	17:18	43° 38,70' N	007° 13,99' E	118	SEISREFL
			02.06.16	17:32	43° 38,49' N	007° 12,45' E	140,2	SEISREFL
			02.06.16	17:42	43° 38,42' N	007° 13,44' E	127,5	SEISREFL
			02.06.16	18:01	43° 38,63' N	007° 12,63' E	26,9	SEISREFL
			02.06.16	18:56	43° 38,32' N	007° 14,00' E	286,9	SEISREFL
			02.06.16	19:10	43° 38,01' N	007° 14,31' E	24,4	SEISREFL
		End	02.06.16	19:28	43° 37,51' N	007° 14,43' E	8,4	SEISREFL
21561-1	POS500_253-1	Start	03.06.16	06:11	43° 38,73' N	007° 13,24' E	12,7	MEBO OBSERV.
		Bottom	03.06.16	06:13	43° 38,73' N	007° 13,24' E	13	MEBO OBSERV.
		End	03.06.16	11:10	43° 38,73' N	007° 13,25' E	13,2	MEBO OBSERV.
21562-1	POS500_254-1	Start	03.06.16	11:58	43° 38,52' N	007° 13,23' E	68,6	SEISREFL
			03.06.16	12:37	43° 38,28' N	007° 14,04' E	317,5	SEISREFL
			03.06.16	13:15	43° 38,83' N	007° 13,95' E	126,2	SEISREFL
			03.06.16	19:37	43° 38,20' N	007° 13,32' E	390	SEISREFL
		End	03.06.16	19:48	43° 37,98' N	007° 14,52' E	488	SEISREFL
21563-1	POS500_254-2	Start	04.06.16	06:01	43° 38,73' N	007° 13,26' E	16	MEBO OBSERV.
		End	04.06.16	06:04	43° 38,74' N	007° 13,24' E	12,6	MEBO OBSERV.
21564-1	POS500_255-1	Start	04.06.16	06:36	43° 38,44' N	007° 13,53' E	131,2	SEISREFL
			04.06.16	06:59	43° 38,59' N	007° 13,94' E	153,7	SEISREFL
			04.06.16	14:23	43° 38,36' N	007° 13,87' E	224,6	SEISREFL
			04.06.16	14:44	43° 39,05' N	007° 14,82' E	275,6	SEISREFL
			04.06.16	17:50	43° 38,56' N	007° 12,71' E	34,5	SEISREFL
			04.06.16	18:03	43° 38,59' N	007° 13,25' E	0	SEISREFL
		End	04.06.16	18:19	43° 38,43' N	007° 13,71' E	0	SEISREFL
21565-1	POS500_256-1	Bottom	05.06.16	06:04	43° 38,77' N	007° 12,94' E	36,2	GC
21566-1	POS500_256-2	Bottom	05.06.16	06:40	43° 38,59' N	007° 12,58' E	17,5	GC
21567-1	POS500_256-3	Bottom	05.06.16	07:12	43° 38,59' N	007° 13,19' E	31,5	GC
21568-1	POS500_257-1	Bottom	05.06.16	07:42	43° 38,74' N	007° 13,27' E	12,5	MEBO OBSERV. Recovery of GeoB21563-1
21569-1	POS500_258-1	Start	08.06.16	13:11	36° 26,28' N	002° 45,79' W	866,3	CTD
21570-1	POS500_258-2	Bottom	08.06.16	14:39	36° 26,30' N	002° 45,80' W	871,1	MEBO OBSERV.
21571-1	POS500_258-3	Bottom	08.06.16	14:47	36° 26,27' N	002° 45,78' W	866,3	MEBO OBSERV.

Gear abbreviations:

AUV	Autonomous Underwater Vehicle
CTD	Conductivity, Temperature, Density sensor
NB+CTD	Niskin bottle + Conductivity, Temperature, Density sensor
GC	Gravity Corer
MEBO OBS. 2015	Recovery of MeBo long-term observatory deployed in 2015
MEBO OBSERV.	MeBo (long-term) observatory
MIC	Mini-Corer
MIC + CTD	Mini-Corer + Conductivity, Temperature, Density sensor
SEISREFL	Seismic reflection profile

From report No. 289 onwards this series is published under the new title:
Berichte aus dem MARUM und dem Fachbereich Geowissenschaften der Universität Bremen
A complete list of all publications of this series from no. 1 to 292 (1986 – 2012) was printed at last in issue no. 292.

No. 289 – Mohtadi, M. and cruise participants (2012). Report and preliminary results of RV SONNE Cruise SO 223T. TransGeoBiOc. Pusan – Suva, 09.09.2012 – 08.10.2012. 47 pages.
No. 290 – Hebbeln, D., Wienberg, C. and cruise participants (2012). Report and preliminary results of R/V Maria S. Merian cruise MSM20-4. WACOM – West-Atlantic Cold-water Corals Ecosystems: The West Side Story. Bridgetown – Freeport, 14 March – 7 April 2012. 120 pages.
No. 291 – Sahling, H. and cruise participants (2012). R/V Heincke Cruise Report HE-387. Gas emissions at the Svalbard continental margin. Longyearbyen – Bremerhaven, 20 August – 16 September 2012. 170 pages.
No. 292 – Pichler, T., Häusler, S. and Tsuonis, G. (2013). Abstracts of the 3rd International Workshop "Research in Shallow Marine and Fresh Water Systems". 134 pages.
No. 293 – Kucera, M. and cruise participants (2013). Cruise report of RV Sonne Cruise SO-226-3. Dip-FIP - The extent and structure of cryptic diversity in morphospecies of planktonic Foraminifera of the Indopacific Warm Pool. Wellington – Kaohsiung, 04.03.2013 - 28.03.2013. 39 pages.
No. 294 – Wienberg, C. and cruise participants (2013). Report and preliminary results of R/V Poseidon cruise P451-2. Practical training cruise onboard R/V Poseidon - From cruise organisation to marine geological sampling: Shipboard training for PhD students on R/V Poseidon in the Gulf of Cádiz, Spain. Portimao – Lisbon, 24 April – 1 May 2013. 65 pages.
No. 295 – Mohtadi, M. and cruise participants (2013). Report and preliminary results of R/V SONNE cruise SO-228, Kaohsiung-Townsville, 04.05.2013-23.06.2013, EISPAC-WESTWIND-SIODP. 107 pages.
No. 296 – Zonneveld, K. and cruise participants (2013). Report and preliminary results of R/V POSEIDON cruise POS448. CAPRICCIO – Calabrian and Adriatic Past River Input and Carbon ConversIOn In the Eastern Mediterranean. Messina – Messina, 6 – 23 March 2013. 47 pages.
No. 297 – Kopf, A. and cruise participants (2013). Report and preliminary results of R/V SONNE cruise SO222. MEMO: MeBo drilling and in situ Long-term Monitoring in the Nankai Trough accretionary complex, Japan. Leg A: Hong Kong, PR China, 09.06.2012 – Nagoya, Japan, 30.06.2012. Leg B: Nagoya, Japan, 04.07.2012 – Pusan, Korea, 18.07.2012. 121 pages.
No. 298 – Fischer, G. and cruise participants (2013). Report and preliminary results of R/V POSEIDON cruise POS445. Las Palmas – Las Palmas, 19.01.2013 – 01.02.2013. 30 pages.
No. 299 – Hanebuth, T.J.J. and cruise participants (2013). CORIBAR – Ice dynamics and meltwater deposits: coring in the Kveithola Trough, NW Barents Sea. Cruise MSM30. 16.07. – 15.08.2013, Tromsø (Norway) – Tromsø (Norway). 74 pages.
No. 300 – Bohrmann, G. and cruise participants (2014). Report and Preliminary Results of R/V POSEIDON Cruise P462, Izmir – Izmir, 28 October – 21 November, 2013. Gas Hydrate Dynamics of Mud Volcanoes in the Submarine Anaximander Mountains (Eastern Mediterranean). 51 pages.
No. 301 – Wefer, G. and cruise participants (2014). Report and preliminary results of R/V SONNE Cruise SO219A, Tohoku-Oki Earthquake – Japan Trench, Yokohama – Yokohama, 08.03.2012 – 06.04.2012. 83 pages.
No. 302 – Meinecke, G. (2014). HROV: Entwicklung und Bau eines hybriden Unterwasserfahrzeugs – Schlussbericht. 10 pages.
No. 303 – Meinecke, G. (2014). Inverse hydroakustische USBL-Navigation mit integrierter Kommunikation – Schlussbericht. 10 pages.
No. 304 – Fischer, G. and cruise participants (2014). Report and preliminary results of R/V POSEIDON cruise POS464, Las Palmas (Canary Islands) – Las Palmas (Canary Islands), 03.02.2014 – 18.02.2014. 29 pages.
No. 305 – Heuer, V.B. and cruise participants (2014). Report and preliminary results of R/V POSEIDON cruise POS450, DARCSEAS II – Deep subseafloor Archaea in the Western Mediterranean Sea: Carbon Cycle, Life Strategies, and Role in Sedimentary Ecosystems, Barcelona (Spain) – Malaga (Spain), April 2 – 13, 2013. 42 pages.
No. 306 – Bohrmann, G. and cruise participants (2015). Report and preliminary results of R/V METEOR cruise M112, Dynamic of Mud Volcanoes and Seeps in the Calabrian Accretionary Prism, Ionian Sea, Catania (Italy) – Catania (Italy), November 6 – December 15, 2014. 217 pages.
No. 307 – Fischer, G. and cruise participants (2015). Report and preliminary results of R/V POSEIDON cruise POS481, Las Palmas (Canary Islands) – Las Palmas (Canary Islands), 15.02.2015 – 03.03.2015. 33 pages.
No. 308 – Wefer, G. and Freudenthal, T. (2016). MeBo200 – Entwicklung und Bau eines ferngesteuerten Bohrgerätes für Kernbohrungen am Meeresboden bis 200 m Bohrteufe, Schlussbericht. 9 pages.
No. 309 – Sahling, H. and cruise participants (2016). R/V POSEIDON cruise POS498, Recovery of Observatories at Athina Mud Volcano, Izmir (Turkey) – Catania (Italy), 18 April – 1 May, 2016. 63 pages.
No. 310 – Fischer, G. and cruise participants (2016). Report and preliminary results of R/V POSEIDON cruise POS495, Las Palmas (Canary Islands) – Las Palmas (Canary Islands), 18.02.2016 – 02.03.2016. 29 pages.
No. 311 – Bohrmann, G. and cruise participants (2016). Report and preliminary results of R/V POSEIDON cruise POS499, Calabrian Mud Volcanoes, Catania (Italy) – Catania (Italy), 04 May – 22 May, 2016. 76 pages.
No. 312 – Kopf, A., Fleischmann, T. and cruise participants (2016). Report and preliminary results of R/V POSEIDON cruise POS500, LISA, Ligurian Slope AUV mapping, gravity coring and seismic reflection, Catania (Italy) – Malaga (Spain), 25.05.2016 – 09.06.2016. 58 pages.